ISTANBUL TECHNICAL UNIVERSITY ★ GRADUATE SCHOOL OF SCIENCE ENGINEERING AND TECHNOLOGY

SYNTHESIS OF COPPER ZINC TIN SULFIDE CZT(S,Se) WITH SOLUTION BASED METHOD AND FORMATION AND CHARACTERIZATION OF CZT(S,Se) THIN FILMS FOR PHOTOVOLTAIC APPLICATION

M.Sc. THESIS

Rıdvan ERĞUN

Department of Nano Science & Nano Engineering

Nano Science & Nano Engineering

MAY 2015

ISTANBUL TECHNICAL UNIVERSITY ★ GRADUATE SCHOOL OF SCIENCE ENGINEERING AND TECHNOLOGY

SYNTHESIS OF COPPER ZINC TIN SULFIDE CZT(S,Se) WITH SOLUTION BASED METHOD: FORMATION AND CHARACTERIZATION OF CZT(S,Se) THIN FILMS FOR PHOTOVOLTAIC APPLICATION

M.Sc. THESIS

Rıdvan ERĞUN
(513111012)

Department of Nano Science & Nano Engineering

Nano Science & Nano Engineering

Thesis Advisor: Doç. Dr. Elif Ülkü ARICI

MAY 2015

İSTANBUL TEKNİK ÜNİVERSİTESİ ★ FEN BİLİMLERİ ENSTİTÜSÜ

SOLÜSYON YÖNTEMİYLE CZTS SENTEZİ VE FOTOVOLTAİK DEVRELER İÇİN CZTS İNCE FİLM OLUŞTURMA VE FİLM ÖZELLİKLERİNİ İNCELEME

YÜKSEK LİSANS TEZİ

Rıdvan ERĞUN
(513111012)

Nano Bilim & Nano Mühendislik Anabilim Dalı

Nano Bilim & Nano Mühendislik

Tez Danışmanı: Doç. Dr. Elif Ülkü ARICI

MAYIS 2015

Rıdvan ERĞUN, a **M.Sc.** student of ITU **Institute of Science and Technology** student ID **513111012** successfully defended the **thesis/dissertation** entitled "**SYNTHESIZE OF COPPER ZINC TIN SULFIDE CZT(S,Se) WITH SOLUTION BASED METHOD: FORMATION AND CHARACTERIZATION OF CZT(S,Se) THIN FILMS FOR PHOTOVOLTAIC APPLICATION**", which he/she prepared after fulfilling the requirements specified in the associated legislations, before the jury whose signatures are below.

Thesis Advisor :	**Assoc. Prof. Dr. Elif Ülkü ARICI** Istanbul Technical University	.....
Jury Members :	**Prof. Dr. Serap GUNES** Yildiz Technical University	.....
	Assoc. Prof. Dr. Hakan KARAAGAC Istanbul Technical University	.....

Date of Submission : 4 May 2015
Date of Defense : 29 May 2015

To my family,

FOREWORD

I would like to special thanks to my thesis advisor Assoc.Prof. Dr. Elif Ülkü ARICI for her guidance, support and motivation.
I also would like to thank to Assoc. Prof..Dr. Hakan KARAAĞAÇ for their helps to complete the characterization works of experiments in laboratories.
I wish my best acknowledgement to Ph.D student Çağdaş ÇALLI for his assistance during my experiments and thesis study.
I also acknowlege to my group friends Amin TABA, Elif PEKSU and Mojgan LAKI for their support.
I would like to express my thanks to
Finally, I would like to thank to The Scientific and Technological Research Council of Turkey (TUBITAK, project number: 111M122) and Istanbul Technical University for their financial support.

May 2015

Rıdvan ERGUN
Material Science & Engineer

TABLE OF CONTENTS

Page

ABBREVIATIONS

CZTS : Cu_2ZnSnS_4

CZTSSe : $Cu_2ZnSnS_xSe_{1-x}$

CIGS : Cu_2InGaS_4

CIS : $CuInS_2$

OLA : Oleylamine

XRD : X-Ray Difraction

EDX : Energy Dispersion of X-Ray Spectroscopy

PCBM : [6,6]-Phenyl C61 butyric acid methyl ester

IPCE : Incident Photon to Converted Electron

GIS : Geographic Information Systems

OPEC : Organization of Petroleum Exporting Countries

IAEA : International Atomic Energy Agency

PV : Photovoltaic

PLD : Pulsed Lased Deposition

KS : Kesterite

ST : Stannite

CH : Chalcopyrite

CA : Cu-Au like

DFT : Density Function Theory

DOS : Density of State

EQE : External Quantum Efficiency

LIST OF TABLES

Page

LIST OF FIGURES

Page

SYNTHESIS OF COPPER ZINC TIN SULFIDE CZT(S,Se) WITH SOLUTION BASED METHOD: FORMATION AND CHARACTERIZATION OF CZT(S,Se) THIN FILMS FOR PHOTOVOLTAIC APPLICATION

SUMMARY

Thin film solar cells are second generation solar cell module. Today's avaliable thin film solar cells suffer from low efficiency of a-Si, shortage of tellerium in structure of CdTe and indium in structure of CIS and toxicity of cadmium in structure of CdTe.

Quaternary $Cu_2ZnSn(SxSe1\text{-}x)_4$ (CZTSSe) compound using an absorber layer in structure of thin film solar cell is considered as a promising candidate for low-cost and high efficiency solar cells because of non-toxic, earth abundant and low cost materials. It can be also synthesized low cost solution based method while other quaternary Cu_2InGaS_4 (CIGS) and ternary $CuInS_2$ (CIS) structure used in thin film solar cell compounds are synthesized expensive vacuum-based technique. This situation make CZT(SSe) more favorable to be used in thin film solar cells as an absorber layer.

CZTS was synthesized with solution-based technique by using precursors which are copper, zinc, tin and sulfur were used for synthesize. Oleylamine (OLA) was used as surfactant and solvent during solution based synthesis. In this study, CZT(SSe) hybrid solar cell structure was occurred.

First step, CZTS was synthesized by using precursors of copper zinc, tin and sulfur precursors which are copper (II) acetylacetonate, zinc acetylacetonate hydrate tin (IV) bis(acetylacetonate) dibromide and elemental sulfur, respectively. These precursors were added at different amount for each synthesis experiment. OLA was used as both solvent and surfactant during synthesis. These precursors were mixed in a flask at determined temperature around 230 ^oC for an hour. After reaction of precursors in OLA, toluene and 2-proponol were added to obtained reaction for washing. Copper poor and zinc rich composition was achieved after several reaction experiments.

Centrifuge process was applied to final supernatant of solution reaction in tubes of 2 ml. It was centrifuged at 12000 rpm for 10 minutes. Supernatant that was wasted from centrifuge was poured with adding toluene and IPA at equal value for next centrifuge step. After solution was completely mixed with ultrasonic bath, it was centrifuged again at 8000 rpm for 20 minutes. After supernatant was completely poured, tubes fill with toluene to be stable ink.

After washing process, final solvent was mixed toluene to make stable CZTS ink. In the second step, CZTS ink in toluene solution was deposited by spin coating method at around 3000 rpm for 1 minute. Quality of films, which were coated at 3000 rpm, was not ideal to be used in absorber layer in thin film solar cell because of non-

continuous film formation. Film uniformity was enhanced by keeping dropped CZTS ink on substrate for few minutes before spinning was started. Heat treatment was applied to coated samples at 175 °C to remove solvent like toluene and 2-propanol (IPA) that added in centrifuge step for each coating step.

Deposited CZTS and CZTSSe layers were characterized with X-Ray diffraction (XRD) and Raman spectroscopy to determine structure of compounds. Not only crystal structure but also composition of CZTS and CZTSSe is important for copper (Cu) poor and zinc (Zn) rich composition, which mostly employed in literature. Therefore, Energy-dispersive X-Ray spectroscopy (EDX) was used to determine composition of annealed samples. Cu/Zn+Sn and Zn/Sn ratio was estimated by EDX characterization. Scanning electron microscopy (SEM) was used to investigate film formation.

Two annealing steps were applied to CZTS coated molybdenum substrate at determined temperature. First annealing process was applied in inert atmosphere on hot plate between 350 °C and 425 °C to define ideal annealing condition. Final compositions of samples that annealed between 350 °C and 425 °C were determined by EDX. They were also characterized by XRD and Raman spectroscopy to determine structure of compounds. UV spectroscopy was used to estimate absorption and transmittance. The UV-vis-NIR absorption spectrum was recorded. Recorded spectrum took the wavelength when the absorption intensity start to take off. Then we can derive the optical band gap using equation: Eg (eV) = 1240/(wavelength in nm).

Annealing processes were applied either to remove surfactant or to enhance crystallization of CZTS grains as a third stage. Even without heat treatment, as-synthesized CZTS film shows that kesterite structure was achieved. Temperature range between 350 ^{o}C and 425 ^{o}C was used to determine ideal heat treatment in nitrogen atmosphere for pure compounds without secondary phases. There was no secondary phases up to 400 ^{o}C. XRD result of sample annealed at 400 ^{o}C showed secondary phases related oxide compound of cations. Annealed sample at 350 ^{o}C and 375 ^{o}C showed the best result in terms of Cu poor and Zn rich compound. Increasing annealing temperature caused to increase composition of Cu compound while composition of Zn compound decrease. Amount of sulfur (S) in CZTS structure decrease during heat treatment at any temperature.

Composition studies show that increasing annealing temperature increase consantration of Cu while decrease consantration of Zn. More annealing temperature means the more loss of S and Zn during annealing process.

Post annealing step was applied to create CZTSSe at determined temperature under selenium (Se) vapor. Selenization was applied to increase formation and crystallization of film. Selenium black 99+ powder was used as selenium source during selenization. Tube furnace was used for selenization. Heat zone of the furnace was determined to locate both selenium powder and samples. Se source was located in tube where temperature was 500 ^{o}C while samples were kept around 350 ^{o}C because evaporated Se vapor can deposit cooler surfaces. Therefore, deposition rate can be increased by this method. Deposited selenium diffused throughout film and replaced sulfur in CZTS. Therefore, composition of CZTSSe compound was achieved at 500 ^{o}C for 40 minutes.

Hybrid solar cell structure was fabricated as a structure with [6,6]-Phenyl C61 butyric acid methyl ester (PCBM) used n type organic semiconductor. Device

structure was constituted of Mo/CZTS-CZT(SSe)/PCBM/Ag. PCBM was coated on CZTS or CZT(SSe) coated molybdenum to create p-n junction. Silver, which is used forward electrode in solar cell structure, was deposited on PCBM via thermal evaporation method.

Incident photon to converted electron (IPCE) and solar simulator were used to examine solar cell performance. IPCE applies monochromatic light to cell to establish amount of current converted incident photon at determined wavelength. This article deals with the term as a measurement of a device's electrical sensitivity to light. Solar simulator apply light at determined standard to simulate sunlight to detect conventional performance of solar cell. Current (I) versus voltage (V) behavior of a solar cell under simulated sunlight.

To sum up, quaternary CZT(S,Se) compound was achieved successfully with composition of Cu poor and Zn rich. Reaction condition was adjusted 230 ^{o}C for an hour in nitrogen atmosphere. We standardized heat treatment at 350 ^{o}C for an hour in nitrogen atmosphere.

SOLÜSYON YÖNTEMİYLE BAKIR, ÇİNKO, KALAY VE SÜLFÜR VEYA SELEN CZT(S,Se) SENTEZİ VE FOTOVOLTAİK DEVRELER İÇİN CZT(S,Se) İNCE FİLM OLUŞTURMA VE FİLM ÖZELLİKLERİNİ İNCELEME

ÖZET

İnce film güneş pilleri ikinci nesil güneş hücre modülüdür. Günümüzde kullanılabile ince film güneş pilleri amorf silikon güneş hücrelerinin verimsizliği, CdTe fotovoltaik teknolojinde kullanılan telyum (Te) ve CIS fotovoltaik güneş pillerinde kullanılan indiyum (I) elementlerinin kıtlığı ve CdTe fotovoltaik teknolojisinde kullanılan cadmiyumun (Cd) zehirli etkisi ile mücadele etmektedir. Bu sebeplerden ötürü CZTSSe büyük ilgi görmekte ve yakın gelecekte ince film güneş pillerinde soğurucu tabaka olarak kullanılmak üzere CIGS ve CdTe soğurucu tabakasına alternatif olarak büyük bir potansiyele sahiptir.

İnce film güneş pillerinde kullanılan diğer soğurucu tabakalar ile karşılaştırıldığında bakır (Cu), çinko (Zn), kalay (Sn), sülfür (S) ve/veya selen (Se) içeren dörtlü bileşik olan CZT(S,Se) zehirli olmayan, yerkabuğunda bolca bulunan ve düşük maliyetli elementler içermesinden ötürü güneş pillerinin maliyetinin düşürülmesi için oldukça önemlidir. İnce film güneş pillerinde soğurucu tabaka olarak kullanılan dörtlü bileşik $Cu_2ZnSn(S_xSe_{1-x})_4$ (CZTSSe) yüksek verim potansiyeli ve üretiminin ucuz olması sebebiyle yakın geleceğin alternatif soğurucu tabakası olarak yüksek ilgi görmektedir. En yüksek verim ile çalışan güneş pillerinde kullanılan CIS ve CIGS soğurucu tabakası vakum yöntemleriyle üretilirken, şu ana kadarki üretilen en yüksek verimlilikle çalışan CZT(S,Se) soğurucu tabakası solüsyon yöntemiyle üretilmiştir. Bu durum CZTS soğurucu tabakasının üretim maliyetini düşürmesinden dolayı bu dörtlü bileşik ince filmlerde kullanılabilmesi açısından önemli yere sahiptir.

CZTSSe dörtlü bileşiğinin yapısını açıklamak için ikili CdTe zincblende kristal yapısına adapte olmuştur. CIS gibi üçlü sistemler CdTe yapısının iki grup II atomunun grup I ve grup III atomuyla yerdeğiştirmesi ile mümkündür. CZTS gibi dörtlü bileşikler, üçlü bileşiklerdeki grup III'teki iki atomun grup II ve Grup IV ile yer değiştirmesi sonucu eldeedilebilir. Bu dörtlüfazlar bir çok kristal yapıda bulunabilmesine karşın güneş pilleri için uygun olan kesterit yapısı termodinamik olarak en kararlısıdır.

Solüsyon yöntemiyle sentezlediğimiz CZT(S,Se) soğurucu tabakası için Cu, Zn, Sn ve S başlangıç malzemeleri kullanıldı. Oleylamine sadece çözücü olarak değil ayrıca reaksyonun gerçekleşebilmesi için yüzey aktif madde olarak da kullanıldı. Bu çalışma sırasında, CZT(S,Se) soğurucu tapakası hibrit güneş pilleri yapısında başarılı şekilde kullanıldı.

Sırasıyla Cu, Zn, Sn ve se S kaynağı olarak kullanılan Copper(II) asetilasetonat, zinc asetilasetonat hidrat and tin(IV) bis(asetilasetonat) dibromide ve elementel sülfürün karışımıyla sentezlendi. Bu bileşenler farklı mollerde karıştırılarak çeşitli sentezler

yapıldı. OLA çözücü ve yüzey aktif malzeme olarak kullanıldı. OLA çeşitli organiklerin uzaklaştırılması için 130 ^{o}C 30 dakika bekletildikten sonra belli oranlarda karıştırılan başlangıç malzemeleri 230 ^{o}C dereceye azot atmosferinde karıştırılan OLA çözeltisine ani olarak eklendi. 230 ^{o}C derecede bir saat karıştırıldıktan sonra toluen ve izopropanol eklenerek yıkama aşamasına geçildi.

Tolüen ve IPA eklenmis son reaksyon tamamen karışana kadar karıştırıldıktan sonra 14000 rpm hızında 10 dakika süre ile santrifüj edilmek üzeere 2 mililitrelik santrifüj kaplarına doldurduldu. Merkezkaç kuvvetinin etkisiyle çöken CZTS tozlarından arda kalan atık sıvı boşaltıldıktan sonra çöken tozlara eşit miktarda tolüen ve IPA eklenerek tekrar 8000 rpm hızında 20 dakika süreliğine santrifüjişlemine maruz bırakıldı.çökeltinin üstünde yüzen solvet çok miktarda nano boyutlu CZTS molekülleri içerdiği için santrifüj yapılamk üzere bir kapta saklandı. Son çökeltiye tolüen eklenip sesötesi banyo uygulanarak çökeltinin tolüen içinde iyice dağılması sağlandıktan sonra kararlı çözelti haline getirildi. Böylece CZTS molekülleri tolüen içinde dağılarak spin kaplama yöntemiyle kaplanması için hazır hale getirildi.

Toluene içinde dağılmış durumda bulunan CZTS molekülleri bekleme sonucu çökme ihtimaline karşın spin kaplama yöntemi ile altlık malzemesine kaplamak için hazır hale getirmek amacıyla manyetik balık ile CZTS molekülleri iyice dağılana kadar karıştırıldı. Mikro pipet ile manyetik karıştırıcı ile karıştırılan CZTS solüsyonu altlık malzemeye damlatılıp iyice yüzeyde dağılması beklendikten sonra döndürme yöntemiyle 3000 rpm hızla bir dakika süre ile döndürüldü. Çeşitli organik bileşenlerin uzaklaştırılması için 175 ^{o}C derecede bir süreliğine kurutma işlemi yapıldı. Arzu edilen kalınlığa ulaşılana kadar döndürerek kaplama yöntemi tekrarlandı.

Çalışmaların sonucunda arzu edilen kompozisyon ve kristal yapıya ulaşıp ulaşılamadığını tespit edebilmek amacıyla X-Ray Diffraction (XRD), raman spektroskopisi ve energy dispersion X-Ray spectroskopisi kullanıldı. XRD ve raman spektroskopisi kristal yapının tespit edilebilmesi için kullanıldı. Dörtlü bileşiklerin reaksyonu sırasında oluşabilecek ikili ve üçlü bileşiklerin tespiti XRD yöntemi ile kesin olarak belirlemek çok zordur çünkü bu bileşiklerin XRD pikleri birbirine çok yakın olup ayırt edilebilmesi çok zordur. Bu sebeple raman spektroskopisi XRD sonuçlarını doğrulayabilmek için beraberce kullanılır. Bakırca yoksun ve çinko zengin bir kristal yapı oluşturulup oluşturulamadığı ise EDX sonuçları ile tespit edildi.

Oluşturulan ince filmler reaksyon sonucu CZTS oluşturmak için kullanılan organik aktif yüzeyi uzaklaştırmak ve krsital yapıyı geliştirmek için ısıl işlem uygulandı. İdeal ısıl işlem bulunabilmesi amacıyla ince filmler 350 ^{o}C ile 425 ^{o}C arasında bir saat süre ile oksitlenmeyi önlemek için nitrojen atmosferinde tavlama işlemi yapıldı. Tavlama işlemi ısıtma ocağı üzerinde yapıldı. 375 ^{o}C sıcaklığın üzerinde sıcaklık uygulanmaya başlandığında ikincil fazların oluşmaya başladığı gözlendi. Ayrıca bu sıcaklıkta Cu az ve Zn zenginfazının yapısı bozulmaya başladı. Bu sebeplerden ötürü 350 ^{o}C ideal tavlama koşulu olarak belirlendi. Raman sonuçlarına göre, 425 ^{o}C tavlama sıcaklığına çıkıldığında ise CZTS yapısı tamamen bozulmaya başladı.

Film yapısını iyileştirmek ve kristal yapıyı ideal hale getirmek için selenizasyon işlemi uygulandı.selenizasyon işlemi tüp fırın içerisinde oksitlenmeyi önlemekiçin nitrojen atmosferinde uygulandı. Selenizasyon işlemi 500 ^{o}C sıcaklığında 20dk ve 40 dk.. süre ile uygulandı. Selenyum kaynağı olarak Selenium black 99+ tozu kullanıldı. Selen kaynağı tüp fırının 500 ^{o}C ısı alanında tutulurken kaplanıcak olan

CZTS filmler 350 ^{o}C derecelik daha soğuk bölgede tutuldu. Böylece daha sıcak olan selenyum buharının daha soğuk olan yüzetde birikmesinin artırılması hedeflendi. Selenizasyon deneyi ayrıca 550 ^{o}C sıcaklıkta 40 dakika süreyle yapıldı. Aşırıverilen sıcaklık Cu_2Se fazının oluşmasına sebep oldu. Bu durumgösteriyorki selenizasyon prosesi ikincil fazların oluşmasına sebep olabilir ve dolayısıyla işlem dikkatli bir şekilde yapılması gerekiyor.

Oluşturulan yapıların güneş pili devresi haline getirmek için molibden (Mo) kaplı cam üzerine sentezlediğimiz CZTS ile kaplandıktan sonra gerekli ise selenizayon işlemi uygulandı. [6,6]-Phenyl C61 butyric acid methyl ester (PCBM), CZTS kaplı molibdenyum altlık üzerine döndürme yöntemiyle kaplandı. Böylece hibrit güneş pili için p-n ekleme yapısı oluşturulmuş oldu. Gümüş (Ag) ise elektrot olarak PCBM özerine ısıl buharlaştırma yöntemiyle kaplanarak Mo/CZTS,CZT(SSe)/PCBM/Ag hibrit fotovoltaik yapısı oluşturuldu.

Oluşturulan hibrit güneş pili yapısının verimliliğinin ölçülebilmesi için Incident photon to current (IPCE) ve güneş simülatörü kullanıldı. IPCE belirlene dalgaboyu aralığında tek dalgaboyu ışık göndererek gelen tek dalga boyu ışıgın ne kadar fotonu etkileyerek elektrık akımına çevirdiği hesaplanır. Bu işlem günlük ışıktan arındırılmış özel bir ortamda yapılır. Güneş simülatörü ise tek bir dalgaboyu yerine görünebilir dalgaboyu aralığında güneş ışığını canlandırmak için örnek belli bir standart ile belirlenmiş ışığa maruz bırakılır. Güneş ışığına maruz bırakılmış haldeyken verilen voltaja karşılık gelen ölçülen akım okunur ve akım voltaj grafiği oluşturulur. Bu grafik üzerinden verimlilik ile ilgili değerler tespit edilir.

1. INTRODUCTION

Quaternary Cu_2ZnSnS_4 has high potential to be used thin film solar cell structure as an absorber layer instead of binary CdS ternary CIS and quaternary CIGS including rare material Indium (In) and CdTe including both toxic Cadmium (Cd) and rare material Tellurium (Te) in its structure. Therefore, CZTS including earth abundant and non-toxic material is a favorable alternative of these components.

1.1 Purpose of Thesis

This thesis includes synthesis and characterization study of CZTS and formation of CZTSSe structure to be in part of in thin film photovoltaic device as an absorber layer. The aim of study is standardized fabrication of CZTSSe layer and achieve literature in terms of performance characteristics. Besides, hybrid solar cell structure was tried in this study with CZTS and PCBM.

1.2 Literature Review

Developing technology caused to multiple to demand of amount of product in short period of time, so manufacturer needed to energy to increase capacity of product. One of the most common energy source has been petroleum product since community started to need energy. Searching these energy sources and making it available are very complex and expensive processes. These energy searches available in specific area lead to crisis throughout the world like petroleum crisis in 1973 because of disagreement between countries. Therefore, price of the petroleum product always versatile. Even though Organization of Petroleum Exporting Countries (OPEC) determined petroleum prices throughout the universe were founded in 1960, petroleum has still caused crisis.

With continuous developments in technology increases the need of energy irrepressibly. However, they also need the nature unspoiled for next generations and that is necessary that provide energy from renewable sources. Furthermore,

maximum of the oil production has been reached already and that means eventually alternatives should be considered. It is certain that resources of fossil fuels are limited and they have an increasing price trend for decades (Figure 1.1). Many developed countries invest the research and development of clean energy and it is clearly certain that renewable energy resources will replace the fossil fuels in future.

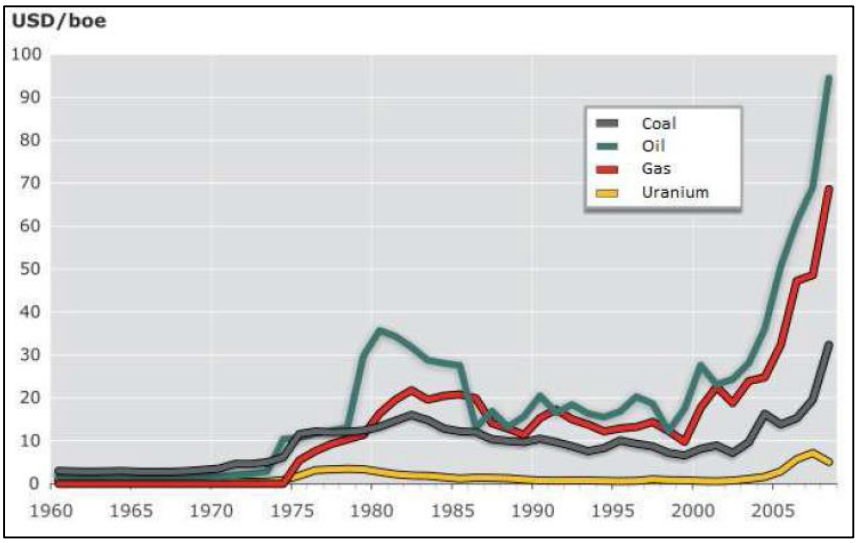

Figure 1.1 : Change in price of non-renewable resources coal, oil, natural gas and uranium [1].

Over use of fossil fuels has caused high carbon emission of atmosphere. Environmental pollution became a current issue. United States met in Kyoto to discuss carbon emission related pollution. Kyoto protocol were singed United Nations Framework Convention on Climate Change in 1997. Government singing this agreement decrease emission of carbon dioxide and five gases, Methane (CH_4), Nitrous oxide (N_2O), hydro fluorocarbons (HFCs), per fluorocarbons (PFCs) and sulfur hexafluoride (SF_6), causing sera effect a level of carbon emission in 1990. Kyoto protocol singing in 1997 came into the operation in 2005 with attendance of Russia because total carbon emission of all these countries had to be decreased level of in 1990 to come into operation. If participant countries continue with emissions above the targets, then they are required to engage in emissions trading; i.e. buying "credits" from other participant countries who are able to exceed their reduction targets in order to offset. The goals of Kyoto were to see participants collectively reducing emissions of greenhouse gases by 5.2% below the emission levels of 1990 by 2012.

In autumn 2013, U.S. Department of Energy published a declaration named "Revolution Now" and they remarked the future roles of four main clean energies and how they are going to achieve their goals for usage of these energies. Many governments have a clean energy policies and goals. Due to these statements and policies clean energy and renewable energy resources are hot topics for the researchers all over the world.

Nuclear energy is also one of the common energy source to generate electricity. In 2011 nuclear power provided 10% of the world's electricity [2]. In 2007, the International Atomic Energy Agensy (IAEA) reported that there were 439 nuclear power reactors in operation in the world,[3] operating in 31 countries. However, Fukushima tragic nuclear accidents are a sequence of events reasoning radioelement emission to atmosphere because of tsunami following Tohoku earthquake occurring in Japan in 2011. This tragic accident caused governments to revise their policy for supplying electric power from nuclear centrals. Germany decided to close temporarily seven nuclear centrals constructed before 1980s to renew. Swaziland also declared that nuclear central plans had been suspended. Argument about presence and use of nuclear centrals spread all over the World. Governments especially European Union tend to research alternative energy.

Limited energy source tend to researcher to study about renewable energy resources such as wind power, hydropower, solar energy, biomass, biofuel and geothermal energy. Photovoltaic (PV) solar energy is one of the important green energy resource. PV solar cells is based electricity conversion from sun light.

Solar cells is a device turning to utilizable electric current from emitted light. PV solar cells has rapidly increasing renewable alternative energy to produce electricity. The first high efficiency solar cell was fabricated Hoffman Electronics creating a 14% efficient solar cell. Following years PV solar cells were used in Telstar space applications.

PV effect was discovered in 1839 but it could not been used in technology effectively until 1950s due to presence of cheap coal and oil. First solar cell (efficiency of 4.5%) was produced in 1954 in United States. PV technologies based on silicon (Si) solar cells have been the focus of research since the 1950s and currently they cover 80- 85% of the PV market globally [4]. Silicon solar cells have

started to pay off during 1980s and solar cells begin to have high attraction thanks to increasing efficiency of silicon solar cells. Green at al. developed 20% efficiency silicon solar cell by using polycrystalline Si wafer in 1985 achieving milestone [5]. However, conventional silicon solar cell archive to reach 15 – 16 % efficiency with polycrystalline Si wafer nowadays [6]. Efficiency of silicon solar cells have increased up to 27% up to now and research is continuing.

Because of some withdraw of Si PV solar cells like, the weight, rigidity, expensive wafer, and processing limitations of Si wafer-based solar cells researchers have interested new materials for PV solar cells. Due to these limitations of Si solar cells, thin film solar cells found a chance to be developed. These thin film PV technologies are based on direct band gap material and high absorption of visible sunlight. Even 2 or 3 μm thickness of thin film solar cells provide high absorption coefficient to absorb nearly all incidental solar light. Besides, thin film solar cells are fabricated with low-cost when compared with production of silicon wafers.

Copper indium gallium selenide solar cells are member of thin film PV solar cell. CIGS cell, sometimes CI(G)S or CIS cell is an inorganic thin film solar cell being members of chalcopyrite family. CIGS solar cell family provide cost-effective electric generation from sunlight. In 2011, 20.3% record efficiency has been shown up to now [7]. Flexible thin film solar cell is also available with CIGS. A world record efficiency of 18.7% on poly imide film has been achieved recently [8], revealing that flexible solar cells with performance close to rigid solar cells can be developed.

There are several fabrication techniques to grow CIGS absorber layer on substrate for high efficiency solar cells. Not only vacuum based methods such as thermal co-evaporation at high substrate temperature or sputtering of precursors on substrate followed by selenization but also non-vacuum technique aiming to reduce cost are mainly used for high efficiency CIGS solar cells. However, expensive vacuum based approach has shown better conventional efficiency when it compared with solution based approach.

Inspite of low cost and non-toxicity of CIGS, rareness of gallium (Ga) and especially indium (In) do not make CIGS usable for a long time. Indium reserves are not inough

to use this element in a solar cell applications. Therefore, new alternative elements have been researched to replace these two elements.

Figure 1.2 shows crystal orientation of quaternary compound. CdTe adopts cubic zinc blende structure as group II – VI compound [9]. Ternary semiconductor I – III – VI_2 structure like CIS can be built by replacing group I and III [10] atoms instead of group II. It is possible to create semiconductor like CZT(S,Se) I_2 – II – IV – VI_4 quaternary by two atoms of group III with group II and IV with octet rule.

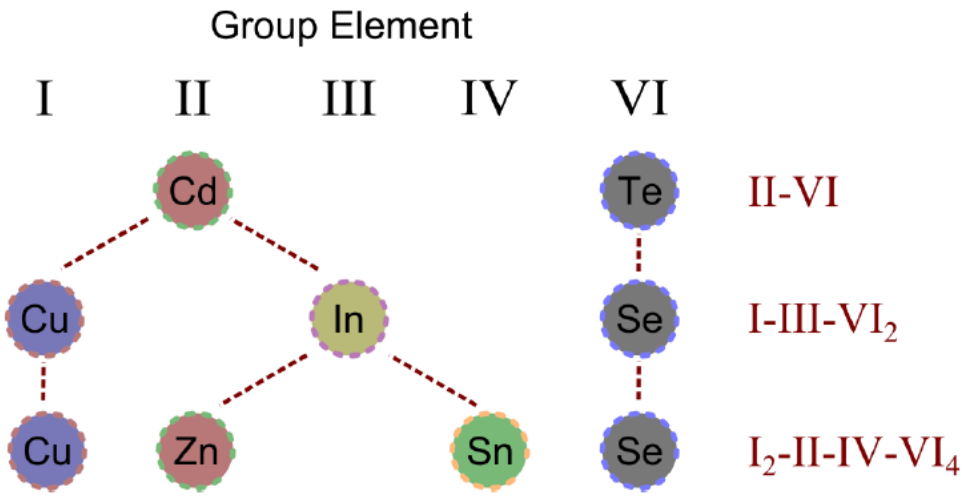

Figure 1.2 : Formation of stoichiometric I_2-II-IV-VI_4 compounds can be achieved by a sequential replacement of cations [9].

There is a recent attention on the absorber materials that are non-toxic, low cost and easily available. It has been achieved with forming Cu_2ZnSnS_4 (CZTS) material in kesterite crystal structure by replacing the two In(III) ion with Zn(II) and Sn(IV). This I_2-II-IV-VI_4 semiconductor has an excellent potential with a band gap of 1.4 - 1.5 eV, a large absorption coefficient of more than 10^4 cm^{-1} and non-toxic and relatively low cost features. All the elements in CZTS absorber are earth abundant and environment friendly. Figure 1.3 shows that the earth crust content and the current world trading price of the elements used in CZTS, CIS and CdTe absorbers. It can be said that the abundance of Zn and Sn in earth's crust is 1500 times and 45 times higher than that of In, respectively, and the price of In is almost two orders of magnitude higher than that of Zn and Sn [11].

Phase diagram of quaternary compound is can be rather complex to display because cations in the structure of quaternary compound can be varied independently from

each other. When we used to say “Cu poor and Zn rich phase” which are commonly employed to describe CZTSSe films, we can be very careful. These terms are intelligible when only one component varies, but when two or more components deviate from stoichiometry, the terminology can be misleading.

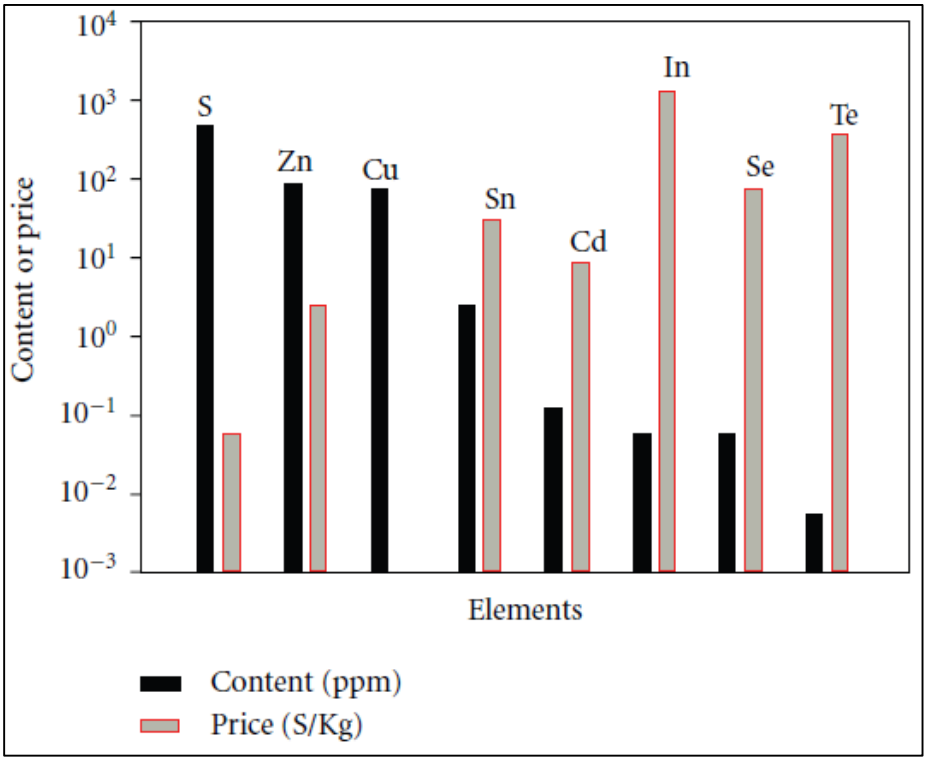

Figure 1.3 : Change in price of non-renewable resources coal, oil, natural gas and uranium.

A comprehensive analysis of the Cu_2X-ZnX-SnX_2 pseudo-ternary system (where X could be S or Se) was carried out by Olekseyuk et al, who presented a phase diagram for the system at 400°C in [13] Figure 1.4. Cu_2ZnSnX_4 as a single phase is present only within a rather narrow range of compositions, which is indicated with an asterisk at the centre of the plot. In all other regions of the phase diagram there are up to two additional secondary phases present, always alongside CZTSSe.

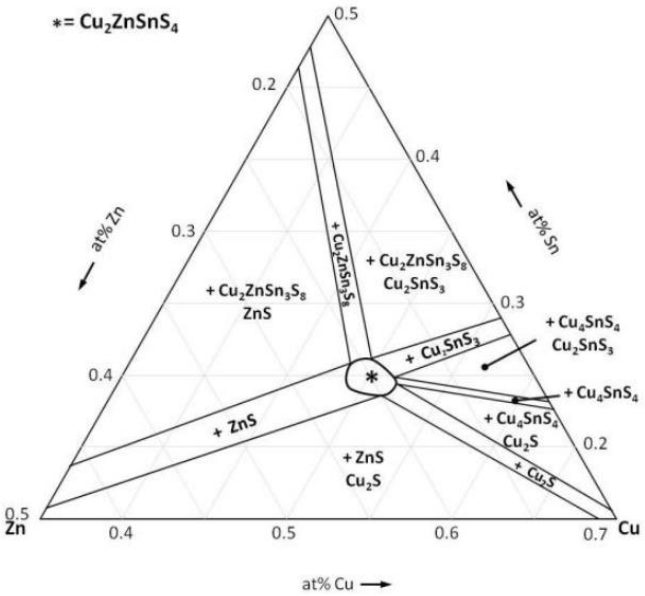

Figure 1.4 : Ternary phase diagrame adapted from reference, showing the expected secondary phases at 400°C [12].

Taking the case of pure CZTS represented in [13] Table 1.1, there are five two-phase fields, in which one secondary phase will be observed in addition to CZTS. In between these there are five three-phase fields, where the secondary phase from both of the bordering regions will be formed alongside CZTS. Other phases not in this diagram but seen during the formation of CZTS in other reports include Cu_4SnS_6 and SnS_2.

Table 1.1 : Defination of composition descriptions used in this report, in terms of the expected secondary phases.

Composition description	Expected secondary phases
"Cu-poor"	$Cu_2ZnSn_3X_8$ + ZnX
"Sn-rich"	$Cu_2ZnSn_3X_8$
"Zn-poor"	Cu-Sn-S + $Cu_2ZnSn_3X_8$ / Cu_2X
"Cu-rich"	Cu_2X
"Sn-poor"	Cu_2X, ZnX
"Zn-rich"	ZnX

The term "Cu poor and Zn rich" is important factor to be formed p type kesterite CZTS structure, but it can be caused secondary phases related this terminology. "Zn rich" phase may cause to be formed zinc sulfide secondary phases, which is have 3.5 eV band gap. This phase behaves as a insulator in CZTS structure because of large bandgap and decreases active area between p-n junction. "Zn poor phase can also form Cu_2S and CTS Cu_2SnS_3 phases which behave as a metallic in structure in CZTS film structure. If CZTS was used as an absorber layer in thin film solar cell with

these secondary phases, two contact may link each other with these phases and device is shunting.SnS_2 phase having n type material properties with a band gap of 2.2 eV [14] can be form in CZTS structure with “Sn rich” composition. Secondary phase of SnS_2 can create p-n junction in CZTS film structure. [15]

There are several methods to synthesize CZTS. Magnetron sputtering deposition [16], electron beam evaporation [17], thermal evaporation [18] pulsed laser deposition [19], sol-gel deposition [20] SILAR method [21] are used to deposit CZTS thin film on substrate. Best efficiency CZTS solar cell was deposited with solution based fabrication [22] instead of highly cost fabrication methods like magnetron sputtering and electron beam deposition [23]. The best efficiency solar cells has been shown by using solution process synthesized by Todorov et. al. [24]. This situation is exactly opposite to synthesizing of CIGS which is reached record efficiencies by vacuum vapor deposition by Philip Jackson [25].

CZTS has significant properties to be used in thin film solar cell applications. To sum up the properties of CZTS materials for thin film solar cell technology:

- CZTS has a p-type semiconductor behavior and can easily create p-n junctions with n-type semiconductor materials like CdS.
- It has a direct band gap and an absorption coefficient more than 10^4 cm^{-1}, which makes it a proper material for thin film photovoltaics applications.
- It has a band gap value of 1.5 eV.
- It is possible to make CZTS solar cells just by replacing CIGS by CZTS in CIGS solar cells.
- Crystallographic structure of CZTS can accept some shifts from the stoichiometric composition.
- It consists of Zn and Si rather than the In and they are produced 20000 and 500 times higher than In, respectively.

Schematic structure and cross section representations of CZTS-based thin film solar cell devices are given in Figure 1.5. It can be seen that CZTS material is found between molybdenum layer and n-type CdS buffer layer to increase crystal orientation between CZTS and TCO (transparant condactive oxite) layer which create p-n junction with p-type absorber layer in thin film solar cell structure [26].

Best efficiency thin film solar cell, which CZTS was used as an absorber layer, has been fabricated with 25 nm CdS buffer layer and 50 nm thickness TCO layer [27].

First PV effect of CZTS material was revealed by Ito and Nakazawa in 1988. They fabricated a hetero-diode that consisted of a transparent cadmium-tin-oxide thin film and a CZTS thin film on a stainless steel substrate [28]. In 1997, Friedlmeier et al. fabricated thin film solar cells using a CZTS layer as the light absorber in contact and a CZTS thin film on a stainless steel substrate [28]. In 1997, Friedlmeier et al. fabricated thin film solar cells using a CZTS layer as the light absorber in contact with an n-CdS/ZnO window layer.

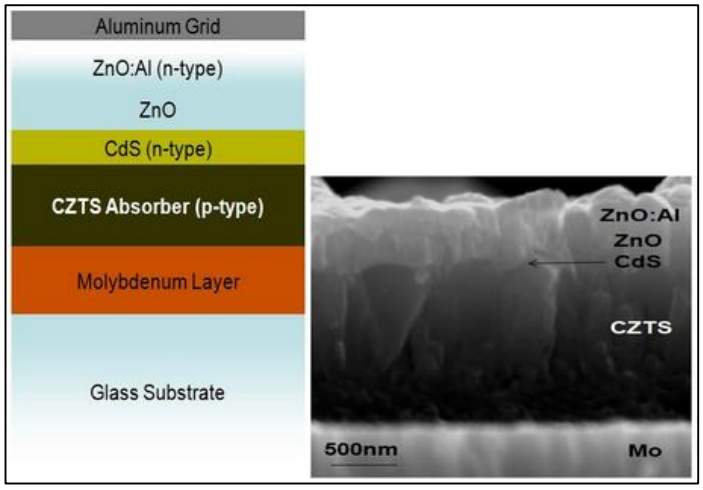

Figure 1.5 : Schematic representation and cross section image of CZTS-based thin film solar cell.

The best energy conversion efficiency produced by the cells was 2.3% [29]. Katagiri et al. had developed this value to 2.63% in 1999. At that study, CZTS film was deposited on a Mo-coated soda lime glass (SLG) substrate [30]. By optimization the process of sulfurization, efficiency of the solar cells was increased to 5.45% and then to 6.7% in 2003 and 2008, respectively [31]. Katagiri and colleagues achieved milestones about the efficiency of CZTS based solar cells in 2005 and in 2009 [32]. In 2010, Todorov et al. have developed a CZTS-based thin film solar with an efficiency value of 9.6% [33]. Figure 1.6 summarizes the change in efficiency values of studies about CZTS based solar cells with years.

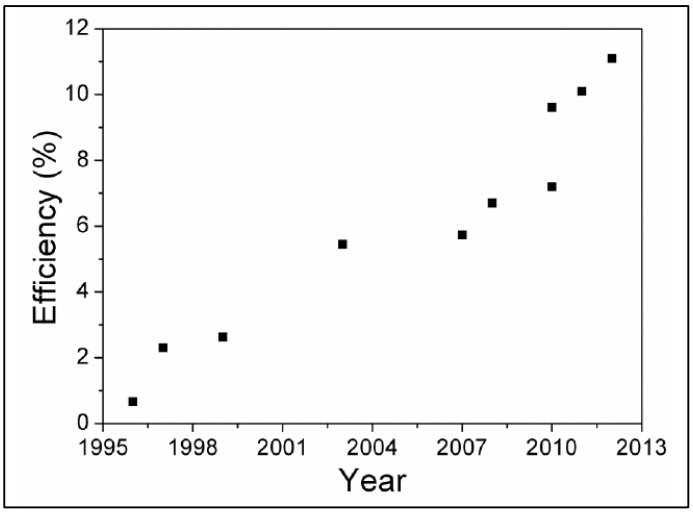

Figure 1.6 : Evolution of efficiencies achieved with CZTS based thin films solar cells.

Hybrid solar cells are combine of organics and inorganics in solar cell structures shown in Figure 1.7. Hybrid solar cell structure CZTS and [6,6]-Phenyl C61 butyric acid methyl ester (PCBM) was studied in this study. Cell structure was prepared in structure of Mo/CZTS/PCBM/Ag. This cell structure has not been studied with CZTS in literature. There is no results for this type of photovoltaics.

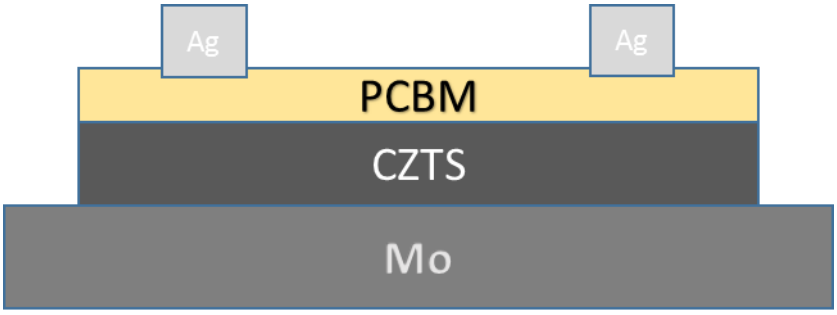

Figure 1.7 : Hybrid photovoltaic structure.

PCBM is known fullerene C_{60} [6,6]-phenyl-C61-butyric acid methyl ester. It is highly used in inorganic solar cells. C_{60} was first synthesized in the 1990s by Fred Wudl's group [34]. It is used as an electron acceptor in organic and flexible solar cells with CIGS.

2. SYNTHESIS METHODS

There are several synthesis methods for creating CZTS absorber layers such as sputtering, evaporation, laser deposition, electrochemical and spin coating. All of these methods can be summarized as two major categories as vacuum based and non-vacuum solution based process.

2.1 Vacuum Based Technique

Vacuum-based techniques mainly involve the deposition of CZTSSe constituents such as metal or binary chalcogenides on substrates under certain temperature and low pressure. These techniques are sputtering, evaporation and laser pulse deposition. Metal targets are used to deposit on substrate at determined sequence and substrate is heated in these techniques. The main advantages of these techniques are high controllable and clear reaction environment.

2.1.1 Sputtering

Physical vapor deposition method, which can be named as sputtering deposition technique, includes deposition of cations via accelerated ion bombardment throughout target material. Metal cations or its binary compound with sulphur are used as a source target. DC magnetic field, RF, hybrid and reactive magnetic sputtering.

In 1988, Iko et al. [28] first reported on the deposition of CZTS thin films using the argon beam sputtering from the pressed target composed of Cu-Zn-Son-S. They deposited CZTS thin film, which has band gap energy of 1.45 eV with kesterite structure. In 2003, Seol et al. have used Copper sulfur (Cu_2S), zinc sulfur (ZnS) and tin sulfur (SnS_2) as target sources to deposit CZTS precursor thin films onto a glass substrate at room temperature by a radio frequency (RF) magnetron sputtering technique. The as-deposited films were amorphous and stoichiometric ratio of Cu/Zn/Sn was achieved after annealing. However, sulfur was missing. After that, this problem was solved by further annealing the films in a sulfur vapor atmosphere at

temperature above 200 °C [35]. RF magnetron sputtering technique with an integrated vacuum apparatus and with sulfurization process is much better process to achieve higher quality and reproducible CZTS films. Moreover, using deionized water to eliminate metal oxide impurity in the CZTS films improves efficiency of solar cells to value of 6.7%. [31]. Hybrid sputtering approach was used by Tanaka and colleagues to deposit Cu, Zn, Sn on a quartz substrate. Drect current (DC) sputtering was used to deposit Sn and Zn layers and RF-sputtering was used to deposit Cu metal layer. Stoichiometry CZTS thin films were formed at the temperature above 400 °C [36]. Liu et al. claimed that CZTS films having high light absorption coefficient ($>10^5$ cm^{-1}) which were synthesized by DC magnetron sputtering technique. They also used a source target consisting of Cu/Zn/Sn metal mixture (Cu:Zn:Sn=2:1:1, molar ratio). Besides the good features of CZTS material, some secondary phases were observed in the materials [37].

2.1.2 Evaporation method

Evaporation method is a deposition technique that metal cations Cu, Zn and Sn deposit on heated substrate by evaporation via applied voltrage. Electron beam evaporation and co-evaporation have been widely used for deposition of CZTSSe thin films.

The first publication on evaporated CZTS thin films was in 1997 by Katagiri et al. by electron beam evaporation with a substrate temperature at 150 °C. [38]. They synthesized CZTS thin film by stacking order of Zn/Sn/Cu (top) which were sulfurized at 500 ℃ under N_2 + H_2S (5 %) atmosphere. They have reached 0.66% conventional efficiency by glass/Mo/CZTS/CdS/ZnO/Al device structure. Katagiri et al. [39] increased conventional efficiency to 2.62% by both replacing of stacking Zn layer with ZnS layer and increasing annealing temperature from 500 to 550 ℃. Kobayashi et al. [40] increased conventional efficiency to 4.53% by changing the stack order to Zn/Cu/Sn (top).

For co-evaporation technique, Wang et al. [41] deposited Cu, Zn, Sn and S simultaneously on Mo-coated class which were heated 110 ℃ during the deposition and then annealing process at 540 ℃ for 5 min. in sulfur atmosphere was applied. They reached 6.8% conventional efficiency by cell structure of glass/Mo/CZTS/CdS/i-ZnO/ITO/ Ni–Al. By increasing annealing temperature from

540 to 570 ℃, Shin et al. [42] reached 8.4% conventional efficiency. Shin et al. [43] also employed TiN barrier layer to helpful in preventing the formation of $MoSe_2$ at the back contact and they demonstrated 8.9 % efficient CZTSe-based solar cells.

2.1.3 Pulsed laser deposition

High quality films with complex compositions can be deposited by pulsed laser deposition technique because of its unique features. Advantages and consequences of deposition by using pulsed laser deposition (PLD) technique can be given such as suitable transfer between the target and deposited films, high energetic species which cause crystallinity enhancement, clean deposition due to absence of atmospheric gas, simplicity and flexibility in the engineering design [44]. PLD is a versatile technique and has so many parameters that affect the film properties such as pulse repetition rate, pulse length, target-to-substrate distance, substrate temperature and orientation [45]. Besides all of these advantages, there are slightly less researches about CZTS solar cells via PLD technique. One of the main reasons of this situation that the small deposition area (generally 1 cm^2) of PLD technique.

Sekiguchi et al. reported the epitaxial growth of CZTS thin films using PLD technique for the first time. CZTS thin films were grown on GaP substrates using CZTS target pellets and they were synthesized by solid state reaction technique of Cu_2S, ZnS and SnS_2 powders mixed with 1:1:1 molar ratio. The powder sealed inside an evacuated quartz ampoule and kept at 750 °C for 24 h. Metal elements were almost stoichiometric but the films were S poor. CZTS thin film had a direct band gap of 1.5 eV [46]. First CZTS based thin film solar cells were reported by Moriya et al. synthesized films were Cu poor and Sn rich and they had a direct band gap of 1.5 eV. Configuration of solar cell device was set to SLG/Mo/CZTS/CdS/Al:ZnO. Efficiency of this device was reported as 1.74% [47].

2.2 Non-vacuum Based Technique

Different vacuum techniques have been used to form CZTS thin films for the usage for photovoltaic systems. But not being cost efficient, having low material utilization and consuming very high energies caused researchers to investigate alternative techniques. These alternative techniques can be classified under the name of non-vacuum approaches. These techniques are simple, low cost and provide good and

uniform thin films. It is low cost fabrication method because both it does not require expensive vacuum system and there is not much material waste during synthesis step of these methods.

2.2.1 Electrochemical method

Electro deposition (electrochemical deposition) is a promising technique for the preparation of different semiconductors for low costs. It is suitable for both small-scale research applications and large scale industrial applications. It is important that to find optimum electrochemical potential which metal cations can be reduced and unwanted reactions will not occur. Electroplating is a process that uses electrical current to reduce dissolved metal cations so that they form a coherent metal coating on an electrode. These cations are reduced at the cathode to deposit in the metallic, zero valence state.

The first report of CZTS thin film synthesized via electrochemical deposition was studied Scragg et al. [48]. They annealed a metal stack of Cu/Sn/Zn (top) deposited on a molybdenum coated glass substrate at 550 °C for 2 h in sulfur atmosphere. They detected SnS2 secondary phase via XRD results, so the conventional efficiency of CZTS cell was only 0.6%. However, the cell performance was increased up to 3.2% by optimizing both sequential order as Cu/Sn/Cu/Zn (top) and annealing condition [49].

Ahmed et al. [50] deposited Cu/Zn/Sn or Cu/Sn/Zn stacks and then they pre-annealed the stacks at low temperature (210 – 350 °C) under inert gas atmosphere. Pre-annealed samples annealed again at 590 °C for 5-15 min. in sulfur atmosphere. They reached 7.3% by optimizing annealing condition. This is highest efficiencies for the pure CZTS-based solar cells prepared from electro deposition to date.

2.2.2 Solution based synthesize

Solution based synthesize is mostly preferred to produce CZTS thin films because of cost effective and higher performance. Surfactant and cations precursors are used to synthesize. The best efficiency solar cells has been shown by using solution process synthesized by Todorov et. al. [24]. This situation is exactly opposite to synthesizing of CIGS, which is reached record high by vacuum vapor deposition by Philip Jackson [25].

In 2007, Tanaka et al. [51] reported on the synthesis of CZTS thin films by a sol-gel approach. Throughout initial studies, researchers used different surfactants instead of Oleylamine (OLA). Tanaka et al. used copper (II) acetate monohydrate, zinc (II) acetate dihydrate, and tin (II) chloride dehydrate as precursors and 2-methoxyethanol as solvent and monoethanolamine as stabilizer. They reach 1.01% conventional efficiency with Cu/ (Zn + Sn) = 0.87 and Zn/Sn = 1.15 chemical composition by applying an hour at 500 °C annealing process in N_2 + H_2S (5 %) gas atmosphere. By optimizing chemical composition to Cu/(Zn + Sn) = 0.80 and Zn/Sn = 1.15, they multiplied the conventional efficiency of their cell performance from 1.01% to 2.03% [52]. They also optimized annealing condition of their study by setting amount of H_2S in annealing condition as 3%, 5%, 10 % and 20% H_2S + N_2. They observed that 3% H_2S +N_2 annealing condition showed best conventional efficiency at 2.23%. They also note that that 3% H_2S +N_2 annealing condition fabricated the narrowest XRD peaks and largest grain size.

Guo et al. reported the first time that the synthesis of CZTS nanoparticles for the use in solar cells. They prepared nanoparticles by hot injection method. In that study, copper actylacetonate, zinc actylacetonate, tin bis(actylacetonate) dibromide were used as metal sources and heated in oleylamine (OLA) as coordinating solvent at 225 °C for half an hour. For the purpose of synthesize CZTS nanoparticles, elemental sulfur in oleylamine was also injected into the solution. XRD patterns revealed that CZTS particles have a kesterite phase. Furthermore, nanoparticles were slightly copper rich. Then CZTS nanoparticles were drop casted onto Mo coated SLG substrates to prepare CZTS nanoparticle thin films. After that, these films were selenized under selenium vapor at 450 and 500 °C. The solar cell device, which was selenized at 450 °C, had an efficiency of 0.74% and the device selenized at 500 °C had an efficiency of 0.80% [53].

In another study, Sheinhagen et al reported CZTS nano crystals solution based synthesized due to its use in photovoltaic systems. Precipitations of copper acetylacetonate, zinc acetate, tin chloride dehydrate and elemental sulfur was trapped in oleylamine at 280 °C for 1h under an inert atmosphere. Sn rich and S deficient nanocrystals were obtained and they nanocrystals had an optical band gap of 1.3 eV. These nanocrystals were used as ink to deposit CZTS layer by spray coating of

toluene dispersion. The configuration of device was set as Au/CZTS/CdS/ZnO/ITO and exhibited an efficiency of 0.23% [54].

Ki et al. [55] fabricated CZTSe thin film solar cell by ink process. $Cu(CH_3COO)_2 \cdot H_2O$, $ZnCl_2$, $SnCl_2 \cdot 2H_2O$ and thiourea are used as a precursors and dimethyl sulfoxide is used as a surfactant. They applied 2 step annealing process i) pre-annealing at 580 °C for 2.5 min. between each spin-coating step in glove box and ii) post-annealing at 500 °C in Se containing atmosphere for 20 minutes. Devices which have a configuration of glass/Mo/CZTSSe/CdS/ZnO/ITO/Ni-Al showed efficiencies of 4.1% with the average metal stoichiometry of Cu/(Zn + Sn) and Zn/Sn were 0.80 and 1.13, respectively in the final films.

Fella et al. [56] fabricated CZTSe thin film by both using copper (II) nitrate hemipentahydrate, zinc (II) nitrate hexahydrate and tin (IV) chloride hydrate as precursors, ethanol, and 1, 2-propanediol to dissolve them. They used knife coating technique to coat film on Mo-coated glass. Coated films were annealed in Se containing atmosphere with temperature range between 330 °C and 660 °C. They observed that double layer structure with a large grain layer on top and a carbon-rich layer near the back contact. They reached 4.28 % conventional solar cell efficiency.

Guo et al. optimized the chemical composition of CZTS nanoparticles of their earlier study [53]. They also used doctor blade technique to deposit the CZTS thin films from the ink of CZTS nanoparticle dispersed in hexanethiol. CZTSSe thin films were then annealed at 500 °C for 20 min in selenium atmosphere. It was obtained that the double-layered structure with larger grains on top after annealing. They constructed solar cells with these films and achieved an efficiency of 7.2% [57].

Guo et al. enhance device performance up to 9.0% by modifying reaction condition and selenization process. They increased reaction time from half an hour to an hour. They also modify selenization process by applying selenization process for 40 minutes at 500 °C and 15 minutes at 550 °C [58].

In 2010, Todorov et al. [33] from IBM explored a new ink formulation approach using the hydrazine as solvent. In this approach, Cu_2S, SnSe, Se, S and Zn were used as precursors. Readily dispersible $ZnSe(N_2H_4)$ particles were formed in situ when stoichiometric elemental zinc powder was added the SnSe-Se solution, which act as act as stress-relief and crack-deflection centers during the deposition of CZTSSe thin

films. CZTSSe thin films with Cu/(Zn + Sn) = 0.8 and Zn/Sn = 1.2 were deposited on Mo coated soda lime glass substrates by spin coating the precursor inks followed by annealing on a hot plate at 540 °C. Solar cells fabricated from the resulting CZTSSe thin films. It had a glass/Mo/CZTSSe/CdS/ZnO/ITO/Ni-Al grid structure, showing conversion efficiencies as high as 9.66 % (VOC = 516 mV, JSC = 28.6 mA/cm2, FF = 65%). In 2012, the same group [24] reported 10.1 % efficient CZTSSe-based solar cells. In these devices, an MgF_2 antireflection coating was used on top of the indium tin oxide (ITO) layer to reduce the loss of the light. Devices analysis showed that the dominant interface recombination, short minority carrier lifetime, and high series resistance limited the performance of the devices. Very recently, they have updated the efficiencies to 11.1%, which is the record efficiencies for CZTSSe-based solar cells based on all kinds of methods [22]. todorov at al. has been achieved to increase CZTS based solar cell performance up to 12.4 % conventional efficiency by optimizing thickness of CdS layer used as bufferlayer and TCO layer used as n-type material to create p-n junction of thin film solar cell structure. Thickness of the CdS buffer layer decrease to 25 nm from 60 nm thickness [27].

3. MATERIALS

3.1 Crystal Structure

The ternary I-III-IV chalcopyrites like CIGS, CIS, CGS and CZTS has attract attention for PV solar cell applications the ternary $CuGaX_2$, $CuInX_2$, and the quaternary Cu_2ZnSnX_4 compounds can be obtained through cation mutation of their II-VI analogs. Further mutation can be carried out by replacing, e.g., Ga+In in $Cu(Ga, In)X_2$, by Zn+Sn to form Cu_2ZnSnX_4 quaternary compounds.Artificial neural networks

There are two fundamental $A^I_2B^{II}C^{IV}X^{VI}_4$ ordering which are chalcopyrite (CH) and Cu-Au like (CA). These bond structure is shown Kesterite (KS), stannite (ST) and primitive CA structure modification (PMCA) are type of structure of Cu_2ZnSnS_4. One is the kesterite structure (KS) (space group $I\bar{4}$, Figure 3.1.a), which is derived from the CH structure. The other two are the stannite structure (ST) (space group $I\bar{4}2m$, Figure 3.1.b) and the primitive mixed CA structure (PMCA) (space group $P\bar{4}2m$, $P\bar{4}21m$ and P2, Figure 3.2. a, b and c respectively), both derived from the CA structure. [59, 60]

The mineral Kesterite for Cu_2ZnSnS_4 (CZTS) belongs to the $A^I_2B^{II}C^{IV}X^{VI}_4$ family and A, B, C and X are copper (Cu), zinc (Zn), tin (Sn) and sulfur (S) or Selenium (Se) respectively. There are two fundamental $A^I_2B^{II}C^{IV}X^{VI}_4$ structure which are Kesterite (KS) (Figure 3.1.a) and stannite (ST) (Figure 3.1.b). Because of the cation disorder throughout $A^I_2B^{II}C^{IV}X^{VI}_4$ lattice, these two structure can be shown. The existence of a Cu/Zn disorder on the structural sites 2c and 2d lead to two type $A^I_2B^{II}C^{IV}X^{VI}_4$ structure [59]. Figure 3.1 a and b show two main crystal syructures of CZTS, which is named kesterite and stannite, with position of atoms. Position of atoms change depending on cystal structure.

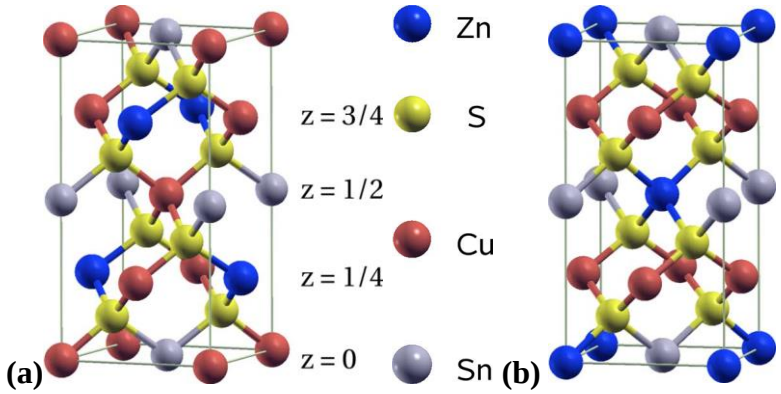

Figure 3.1 : Schematic representations of the (a) kesterite and (b) stannite structures [61].

Different structural modification of CZTS are related alternate cation layer of CuSn, CuZn, CuSn and CuZn at z= 0, ¼, ½ and ¾ respectively [61]. ZnSn layer, the primitive cell being again bct, replaces Cu_2 top layers of Kesterite. Besides, there are three type modifications of kesterite and stannite structure [62]. Due to Cu – Zn disorders, there are three types modification of $A^{I}_2B^{II}C^{IV}X^{VI}_4$ structure shown in Figure 3.2.a. Two Zn and Cu atoms take place their location in KS structure at z= ¼ and this create a "stacking" fault with respect to the bct KS structure. Cu and Zn atoms order at ¾ and ¼ respectively in Figure 3.2.b and 2 Cu atoms are replaced two Zn atoms at z=3/4 in Figure c and this recovers the stannite structure at the layers z= ½ and z= 3/4 , but maintains the kesterite structure in the other two layers. These modifications belong to the tetragonal space groups $P\bar{4}2c$, $P\bar{4}21m$, and P2, respectively [61].

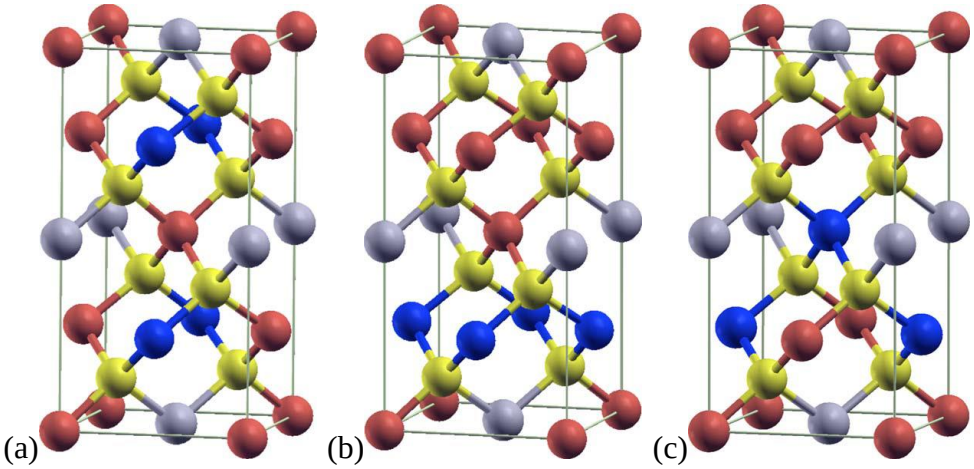

Figure 3.2 : Total energy differences obtained using PBE and HSE [61].

Theoretically, KS structure (space group $I\bar{4}$) is more stable than ST structure for the $Cu^{I}_2Zn^{II}Sn^{IV}S^{VI}_4$ system due to the small strain energy and more negative Madelung

energy [63, 64, 65]. The stannite (ST) structures [space group $I\bar{4}2m$, Figure 3.1.a] are slightly less stable than the kesterite (KS) structures because of energy differences between them which are about 3 meV/Atom [60], and the KS and ST structure ordering may coexist in the synthesized samples[59].

Predicted lattice parameters of kesterite, stannite and three modification of them shown in Figure 3.3. KS type structure which has $I\bar{4}$ symmetry is predicted the most stable I-III-IV structure both for density functional theory (PBE) as well as for hybrid functional HSE, but the $P\bar{4}2c$ modification is very close in energy with $I\bar{4}$ Kesterite structure [60, 61].

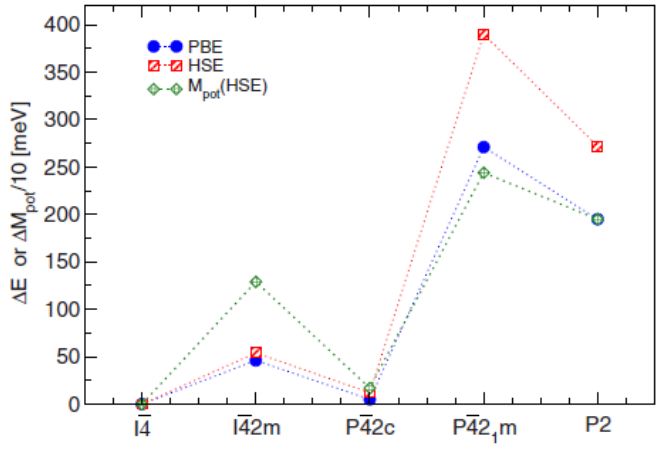

Figure 3.3 : Atomic sphere radii are chosen arbitrarily at hree structural difications of kesterite $P\bar{4}2c$, $P\bar{4}21m$, and P2 space group, respectively [61].

3.2 Electrical Properties

The chalcogens concentration into CZTSSe alloys gives the possibility to make band engineering to tailor the material properties for a given application, but at the same time, allows having some alloy disorder.

Calculations of the electronic band alignment of Cu2ZnSn(SxSe1-x)4 alloys by density functional theory (DFT) reveal a direct bandgap monotonically increasing from 1.0 eV 29 (pure CZTSe) to 1.5 eV (pure CZTS) [60] with a small bowing parameter (b~0.1) as reported in equation 3.1.

$$E_G(x) = (1-x)E_G(CZTSe) + xE_G(CZTS) - bx(1-x) \qquad \textbf{(3.1)}$$

Table 3.1 also shows that band gaps of five modifications by using PBE and HSE estimations. Stannite and two modifications, which are $P\bar{4}21m$ and P2 are predicted to be metals using PBE. HSE gives better information about band gaps and Kesterite and $P\bar{4}2c$ modification are predicted largest band gaps. Kesterite and $P\bar{4}2c$ possess virtually identical band gaps, indicating that cation disorder within the Cu-Zn layer will hardly modify the optical properties, but it may reduce mobility of carriers due to the potential disorder. [61].

$A^{I}_2B^{II}C^{IV}X^{VI}_4$ lattice structure with Se atom is valid for KS, ST and all modification of it. Because of larger radius of selenium atoms the lattice structure of CZTS slightly chance. This affect the electronic properties of Kesterite structure. When we compare band gap of CZTS with CZTSe, band gap of Kesterite structure decrease noticeably from 1.5 eV to about 1 eV.

CZTS as an ionic material associate the following formal valencies with the atoms: Cu^{+}, Zn^{2+}, Sn^{4+}, and S^{2-}. Stannite CFTS which appear $Cu^{2+}Fe^{2+}Sn^{4+}S_4^{2-}$ and CZTS Kesterite structures are similar to each other, so the same arguments may apply to the cationic valencies in CZTS Kesterite with stannite CFTS.

Shiyou Chen et al. calculated density of state (DOS) of stannite and Kesterite structure of CZTS. DOS results of these two structure is very similar due to their similar chemical compositions and structures. Shown isn Figure 3.4. They note that upper valance band consist of mainly from the hybridization of S p and Cu d states. Upper valance band also derived from same states in CIS and $CuGaSe_2$ (CGS) because Cu has higher d orbital energy than other cations in CZTS, CIS and CGS [60].

Table 3.1 shows that crystal parameter and stability of different krystal structure of CZTS and CZTSSe. Gibbs free energy of KS phase is higher than oter alternative phases. Therefore, KS struructure of CZTS and CZTSe is the most staple phase when they compeared with ST and PMCA structure thermodimaically. Gibbs free energy of KS structure in CZTSSe phase is closer the others when compeared with KS structure in CZTS.

Table 3.1 : Lattice parameters a_0, b_0, and c_0 (in Å) of modifications of CZTS as obtained using density functional theory (PBE) and hybrid functional (HSE) compared to experimental values.

Type		Kesterite		Stannite		Modifications					
Symmetr		$I\bar{4}$		$I\bar{4}2m$		$P\bar{4}2c$		$P\bar{4}21m$		P2	
	Expt.	PBE	HSE	PBE	HSE	PBE	HSE	PBE	HSE	PBE	HSE
a_0 (Å)	5.427[a]	5.466	5.466	5.460	5.438	5.466	5.446	5.478	5.464	5.473	5.443
b_0 (Å)										5.478	5.452
c_0 (Å)	10.871[a]	10.929	10.889	10.976	10.941	10.929	10.885	10.942	10.857	10.939	10.892
$c_0/2\ a_0$	1.001	1.000	0.999	1.005	1.006	1.000	0.999	0.999	0.993	0,999	1,001
Δ E		0.0	0.0	0.046	0.054	0.005	0.012	0.271	0.390	0.195	0,277
E_g (eV)	1.44–1.51[b]	0.096	1.487	−0.030	1.295	0.071	1.458	−0.097	1.206	−0.111	1.073

Table 3.2 : Lattice parameters a_0, b_0, and c_0 (in Å) of CZTS and CZTSe.

Ref.	Structure	a Å	η	Δ_{CF} (eV)	Δ (meV)	E_g (eV)
				CZTS		
	KS	5.467	0.999	-0.065	0	0.09 (1.50)
[60]	ST	5.458	1.004	0.138	2.86	-0.3 (1.38)
	PMCA	5.459	1.005	0.128	3.15	-0.06 (1.35)
				CZTSe		
	KS	5.763	0.998	-0.031	0	-0.30 (0.96)
[60]	ST	5.762	1.000	0.066	3.79	-0.44 (0.82)
	PMCA	5.753	1.004	0.065	5.53	-0.47 (0.79)

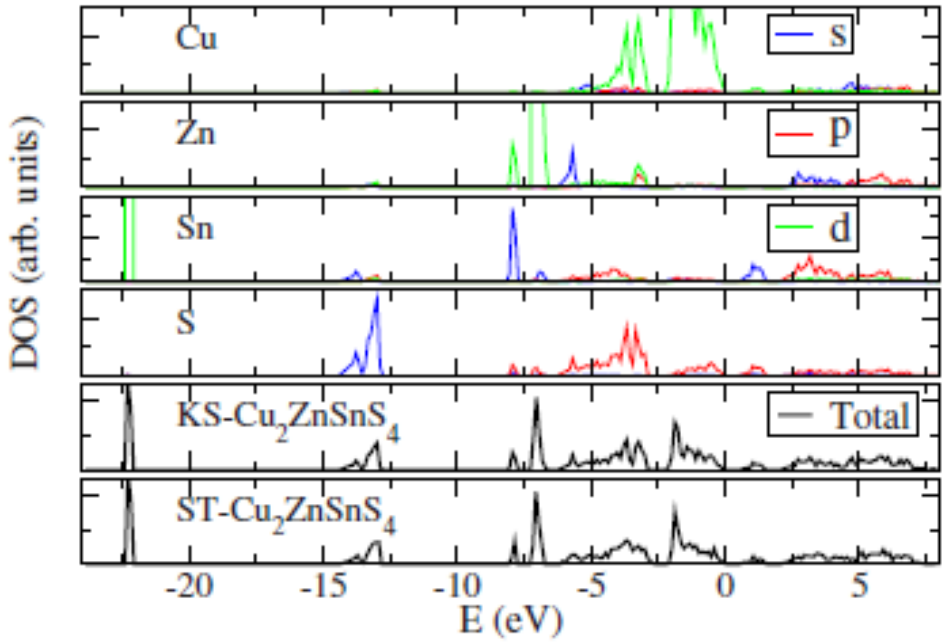

Figure 3.4 : The partial and total DOS of Cu_2ZnSnS_4 in KS and ST structures and the partial DOS in the KS structure [61].

The upper valence band is derived mainly from the hybridization of S p and Cu d states, similar to $CuInSe_2$ and $CuGaSe_2$. Cu has higher d orbital energy than Zn, Ga, In, and Sn, while the low conduction band is mainly from the hybridization of S s p and Sn s states, which is due to the lower s orbital energy of Sn than the other cations. [61] Figure 3.5 shows that DOS of CZTS structure. The S-3s and S-3p states are clearly visible at −14 to −13 eV and −6 to −3 eV, respectively. The Zn-3d states form a very narrow band located −7 eV below the Fermi level, and the valence band is clearly made up of Cu-3d states (−2 to 0 eV) [61].

Paier et. al. illustrate valance and conduction band of Kesterite CZTS in [61] Figure 3.6. Conduction band maximum consist of bonding and anti-bonding between Cu-3d and S-3p* states below the Fermi level. The first conduction band is made up of the corresponding anti-bonding linear combination of Sn-5s and S-3p (Sn-5s /S-3p*) states. This covalent picture, the electronic charge density arising from the band located at −7 eV (Sn-5s /S-3p), and the charge density corresponding to the first conduction band (Sn-5s /S-3p*) are shown in Figure 3.6.

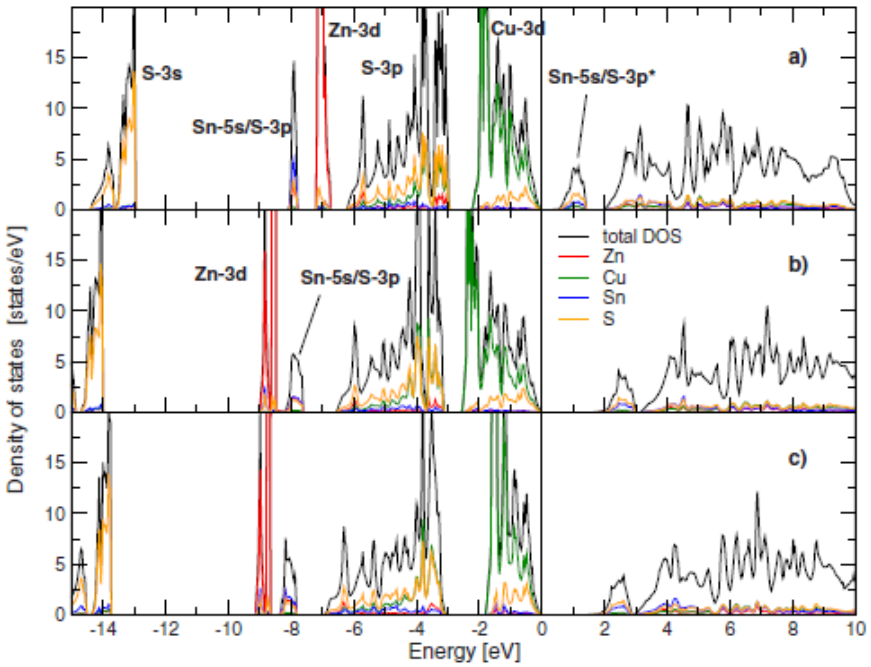

Figure 3.5 : Total and orbital project density of states of CZTS kesterite calculated using (a) PBE, (b) HSE, and (c) G_0W_0 (HSE) [61].

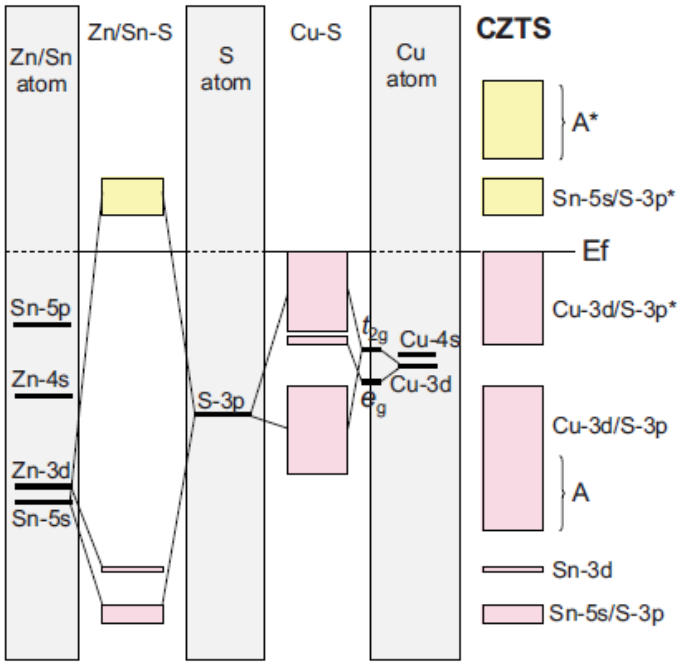

Figure 3.6 : Molecular interaction diagram schematically illustrating the atomic one-electron energies and the band structure of CZTS [61].

Lui et al. note from [65] Table 3.3 and table 3.2 that the electron effective masses are isotropic, while the hole effective masses show strong anisotropy, and the electron effective masses are typically much smaller than the hole effective masses for all studied quaternary semiconductors [65]. Hole masses are about three times larger

than that of the longitudinal hole mass in these materials. This difference between the electron and the hole effective masses could be understood by analyzing the constituents of the conduction band maximum and the valance band minimum shown in [65] Figure 3.5. For the conduction band maximum, a notable contribution from the spherically symmetric s states of the Sn element is observed, which could account for the small isotropic electron effective masses. On the other hand, the valance band minimum is dominated by the low-lying anisotropic d states of Cu atoms and p states of the anions, which could lead to the large anisotropic hole masses.

Table 3.3 : The Γ point electron effective masses (mc) and hole effective masses calculated from band-energy dispersion [65].

	Cu_2ZnSnS_4	
	Kesterite	Stannite
$m^{\parallel}_{c1}$⊥	0.18	0.18
m⊥$_{c1}$	0.19	0.19
$m^{\parallel}_{v1}$	0.22	0.74
m⊥$_{v1}$	0.74	0.34
$m^{\parallel}_{v2}$	0.65	0.69
m⊥$_{v2}$	0.34	0.32
$m^{\parallel}_{v3}$	0.66	0.20
m⊥$_{v3}$	0.30	0.69

Selenium addition instead of sulfur atoms in CZTS structure, do not chance conduction process. It can be clearly seen that the DOS of the KS and ST structure which are quite similar the upper valence bands. It is mainly derived from the hybridization between p states from Se atoms and d states from Cu atoms, while the lower conduction bands are mainly derived from the hybridization between the s and p states from Se atoms and s states from Sn atoms [65].

The most obvious trending on the effective masses of $Cu_2ZnSn(VI)_4$ (VI = S, Se) in [65] Table 3.3 and Table 3.4 show that the electron and hole effective masses of Se-based compounds are significantly smaller than those of S-based compounds, more precisely. The effective masses of CZTS are around 50%~ 100% larger than those of CZTSe with the same structure. This trend on the effective masses reflects the fact that the lowest conduction band (CB) and topmost valence band (VB) of Se-based compounds have stronger downward and upward energy dispersions around the Γ point than those of S-based compounds, which also contributes to the smaller gaps in [60, 65] Table 3.2.

Table 3.4 : The Γ point electron effective masses (mc) and hole effective masses calculated from the band-energy dispersions [65].

	$Cu_2ZnSnSe_4$	
	Kesterite	Stannite
$m^{\parallel}_{c1}$	0.10	0.09
$m^{\perp}_{c1}$	0.11	0.10
$m^{\parallel}_{v1}$	0.12	0.55
$m^{\perp}_{v1}$	0.32	0.14
$m^{\parallel}_{v2}$	0.53	0.13
$m^{\perp}_{v2}$	0.16	0.23
$m^{\parallel}_{v3}$	0.34	0.18
$m^{\perp}_{v3}$	0.26	0.35

Band gap dependence of $Cu_2ZnSn(S_xSe_{1-x})$ according to composizion of x in structure of S and Se is shown in [66] Figure 3.7. Band gap of CZTSSe structure can be adjusted between 1.o eV and 1.5 eV according to rate between S and Se in its structure. Therefore, quaternary compound CZTSSe make enable to band gap engineering of absorber layer.

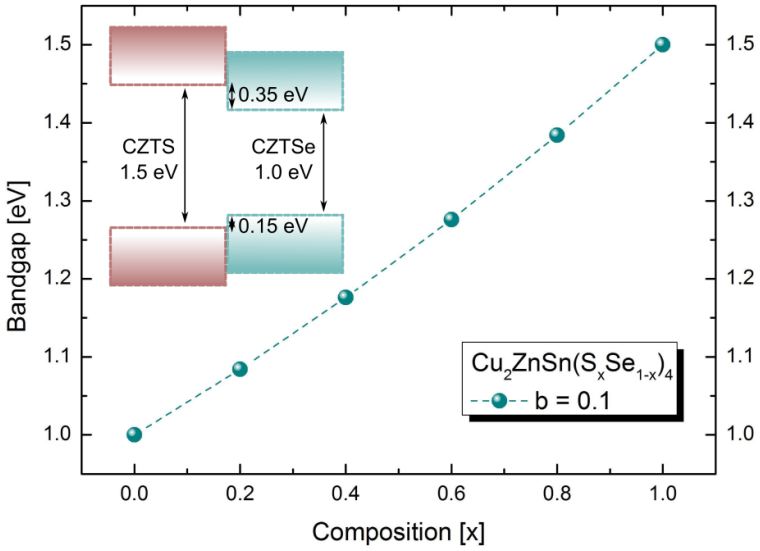

Figure 3.7 : $Cu_2ZnSn(S_xSe_{1-x})$ band gap variation as function of the composition (x) [66].

4. EXPERIMENTAL STUDIES

4.1 Synthesis Process

Hot injection method has been used for this study. It is a method which solution based synthesis includes reaction between precursors with a surfactant in a solvent for synthesizing CZTS ink in inert gas atmosphere.

4.1.1 Precursor materials

Cu(II) acetylacetonate, Zinc acetylacetonate hydrate and tin(IV) bis(acetylacetonate) dibromide were use as cation precursors and elemental sulfur was used as a sulfur source. Oleylamine (OLA), which were purchased from Sigma-Aldrich, was used as a surfactant and solvent. Selenium black 99+, which was purchased from Merck, was used for selenization process.

4.1.2 Senthesis of CZTS ink

Three neck flask 50 ml was used for reaction of precursors. Gas inlet, gas outlet and cooler were adapted to the necks of flask. Gas outlet was affiliated with bubbler for both gas filtration and preventing oxygen inlet. Cooler was used to cool gases, which are mostly sulfur, comprised of reaction to prevent loss of sulfur during reaction. Gas inlet consisted on two part as nitrogen inlet and vacuum exhaust. After air in flask exhausted with vacuum, nitrogen gas was filled to the flask. The reaction system in silicon oil bath was heated with hot plate. Temperature of oil was detected with thermocouple.

Figure 4.1 illustrates that the reaction steps of CZTS. 10 ml OLA was heated to 120 °C in three neck flask to reflux OLA and then the solution was degassed with nitrogen (N_2), after the flask was exhausted by vacuum. After OLA solution was refluxed, it was heated to reaction temperature 230 °C. When the solution reached 230 °C 4.5 ml 1 M sulfur in OLA was injected the heated solution to increase anion concentration. After sulphur was completely mixed in the solution, cations in OLA

solution including 1.332 mmol cu(II) acetylacetonate, 0.79 mmol Zinc acetylacetonate hydrate and 0.75 mmol tin(IV) bis(acetylacetonate) dibromide in 6 ml OLA were added to the solution in 3 neck flask. After the reaction flask was degassed again, the reaction was kept at 230 °C for an hour. Reaction was cooled to room temperature to fill 5 ml toluene. Final solution was stirred for a while. After added toluene was completely mixed, 40 ml isopropanol (IPA) was inserted to the solution.

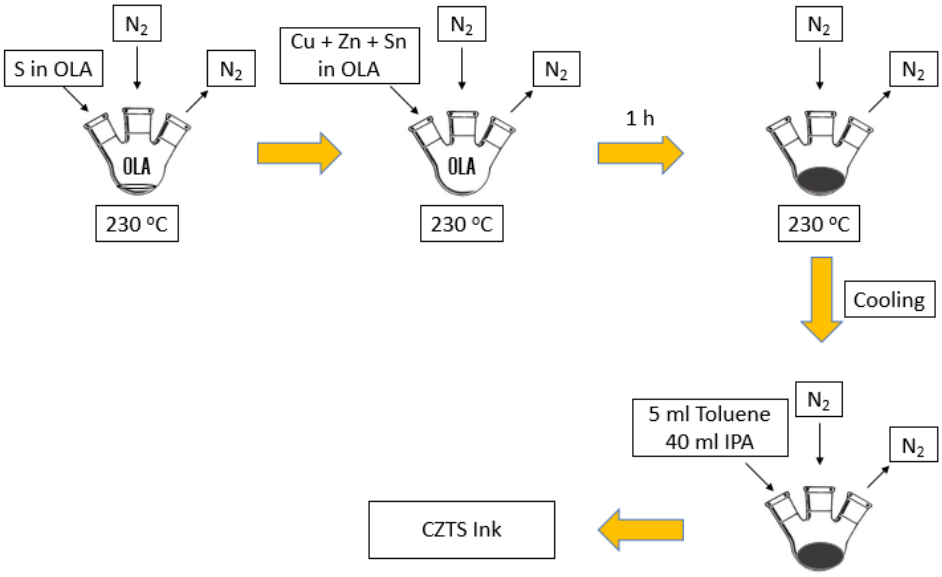

Figure 4.1 : Reaction steps for synthesize CZTS ink.

Final solution was filled to centrifuge tubes, which have 2 ml capacity to centrifuge them. The tubes were firstly centrifuged at 14000 rpm for 10 minutes. Supernatants were poured and filled again with 0.6 ml toluene and 0.3 ml IPA for each one. They were centrifuged again at 10000-rpm for 20 minutes. Final supernatants were collected in a flask. Finally, the centrifuge caps were filled with toluene and collected in a tube as final CZTS inks.

CZTS films were deposited on molybdenum (Mo) coated glass and Mo foils via spin coater at around 3000 rpm for a minute. Before CZTS were coated on Mo films, we have stirred the CZTS solution with magnetic stirrer. Solution was stirred vortexing to precipitate CZTS particles in solution for a while.

Spin coating condition was standardized between 250 and 3000 rpm for one minute. Spinner rolled 500 rpm for 10 seconds after it was rolled 250 rpm for 10 seconds to

precipitate CZTS particles throughout substrate. Finally, rolling speed of spinner has reached to 3000 rpm for 40 seconds.

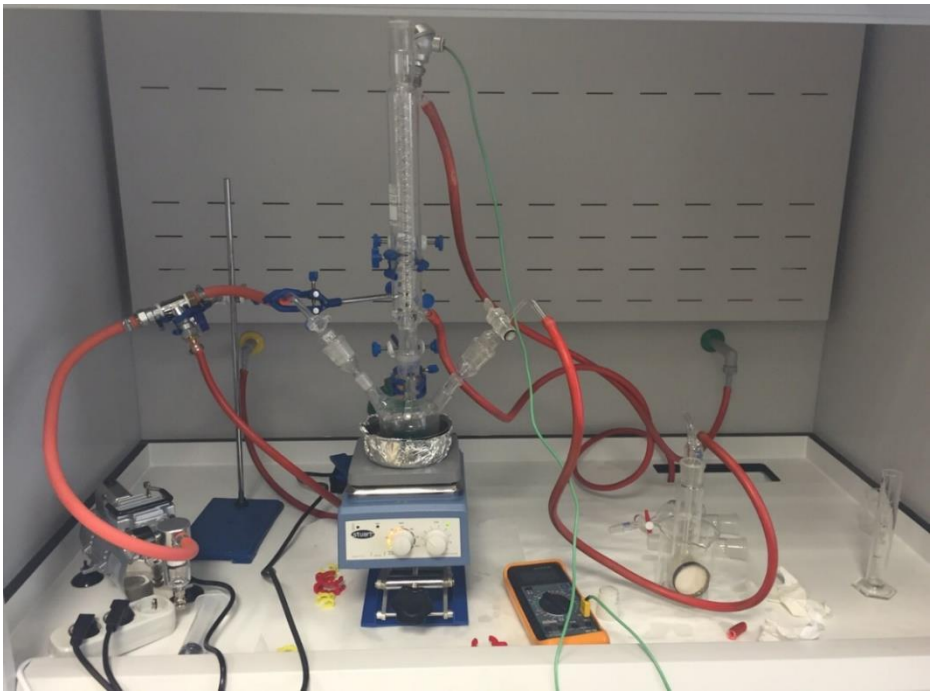

Figure 4.2 : Reaction system for synthesize CZTS ink.

Figure 4.3 shows film thickness dependence on coating steps. Thickness of first spin coating step was estimated around 50 nm. When coating steps were carried on from one to four, thickness of the film has also increased to around 250 nm. After this point, increasing rate of film thickness was enhanced because of interaction between coated CZTS particles on substrate and CZTS ink is stronger than between Mo and CZTS. Each four coating steps is equal to 500 nm after first four steps.

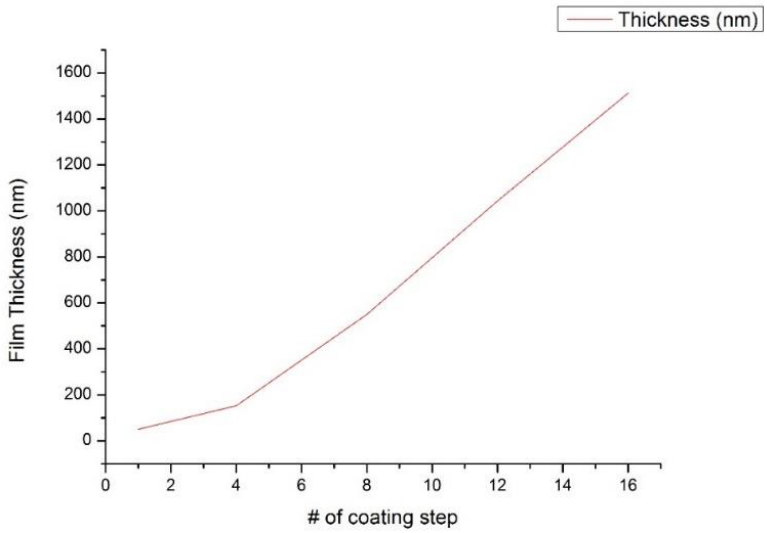

Figure 4.3 : Film thickness dependence on coating steps.

4.2 Heat Treatment

Two step heat treatment, which are annealing and selenization, were applied to remove organics, which was added during synthesis and cleaning step, and to increase crystal stability of CZTS particles on film.

4.2.1 Annealing process

To increase crystallites of CZTS grains, annealing process was applied between 350 °C and 425 °C for an hour as a first step of annealing process to observe ideal annealing condition for optimum crystalinity and composition of CZTS. Daihan Maxtir 500 High Temperature hot plate (Figure 4.4) is used for first annealing step. The samples were put in an oval shaped glass that was placed on the hot plate. Pure nitrogen (N_2) gas also purged during the annealing process to protect to samples from oxidation.

Figure 4.4 : Annealing process.

4.2.2 Selenization process

Selenization process was carried out in Pyrex glass tube. Selenium black 99+ and samples were put in the tube shown in Figure (4.5). Selenium precursor was evaporated at 500 °C for 15 minutes. Evaporated selenium gas deposited on the samples and selenium replaced with sulfur. CZT(S,Se) composition was obtained via selenization process. Waste selenium gas was passed throughout cooling part and filtrated via linen fiber in water.

Figure 4.5 : Tube furnace for selenization process.

4.3 Cell Structure

CZTS ink was deposited on Mo-coated glass by spin coating process which was detailed in section 4.1.2. Mo-coated glasses were cleaned in purified water and acetone solution respectively in ultrasonic bath before coating of CZTS ink on it. Acetone was taken placed by methanol to keep cleaned Mo-coated glasses.

PCBM was deposited on CZTS, which was coated on Mo-coated glass with same spin coating condition when CZTS deposited on Mo-coated glass. Silver contact was deposited on PCBM by thermal evaporator at arount 10^{-6} barr.

Final cell structure was constituted as Mo/CZTS/PCBM/Ag and Mo/CZT(S,Se)/PCBM/Ag. This cell structures were characterized via IPCE and solar simulator.

4.4 Characterization Experiments

This part of thesis includes characterization studies of materials. Structural analysis and composition analysis of CZTS and CZTSSe samples were studied. Cell performance of photovoltaic module was estimated IPCE studied.

4.4.1 Structural analysis

Crystal structures of synthesized CZTS and CZTSSe samples were determined by XRD and Raman spectroscopy experiments. Composition of samples were

determined via EDX experiments at determined experiment conditions. Band gaps of CZTS and CZTSSe films were estimated via UV-vis spectroscopy in our laboratory.

4.4.2 X-Ray diffraction experiment

Different phases in the coatings were identified by the GBC MMA X-Ray Diffractometer. K-alfa radiation was used as X-Ray radiation source during XRD analysis. The measurements were adjusted with 0,02^o angle steps with a speed of 2^o for per minute. The analysis was performed angular rate between 20^o and 90^o.

4.4.3 Raman spectroscopy experiment

Different phases in the coatings CZTS and CZTSSe were identified by Renishaw Invia Raman Microscopy with 633 nm excitation laser sources having %5 intensity with the scanning duration of 60 seconds.

4.4.4 SEM and EDX analysis

Zeiss Ultra Plus Field Emission Scanning Eelectron Microscope was used to determine surface morphology and composition of CZTS and CZTSSe films by using 15 kV high voltage.

4.4.5 UV-visible spectroscopy

Agilent 8453E UV visible spectroscopy device was used at between 200 nm and 1100 nm wavelength range for 30 seconds. UV-vis analysis was performed for CZTS inks and CZTSSe coated glass samples to detect absorbance coefficients and band gaps of the samples.

UV- Visible spectroscopy has calculated the band gap of CZTS and CZTSSe layers by using light source wavelength between 300 nm and 1100 nm. By appliying light between 300 and 1100 nm wavelength, transmition coefficient of films were estimated via drawing $(\alpha h\nu)^2$ versus $h\nu$ graphic. $(\alpha h\nu)^2$ and $h\nu$ were estimated with formula 4.1.

$$(\alpha h\nu)^2 = (-\frac{1}{d}.\ln(T).\frac{1240}{\lambda})^2 \qquad \textbf{(4.1)}$$

$(h\nu)$ was also estimated with formula 4.2.

$$(h\nu) = \frac{1240}{\lambda} \quad \textbf{(4.2)}$$

Drawing graphic of $(\alpha h\nu)^2$ versus $h\nu$ provides to estimate bandgap of samples by normalizing of slope.

4.4.6 Cell Performance Analysis

Hybrid cell structure of Mo/CZTSPCBM/Ag was performed as a photovoltaic device. Quantum efficiency of PV cell structures were displayed at IPCE.

4.4.7 Incident photon to converted electron analysis

The term quantum efficiency (QE) may apply to incident photon to converted electron (IPCE) ratio. Fundementals of IPCE estimate ratio between converted electrons by irridiated photon at determined monochromatic wavelength between 300 nm and 1200 nm.

External Quantum Efficiency (EQE) is the ratio of the number of charge carriers that are collected by the solar cell to the number of photons of a given energy shining on the solar cell from outside (incident photons). Internal Quantum Efficiency (IQE) is the ratio of the number of charge carriers that are collected by the solar cell to the number of photons of a given energy that shine on the solar cell from outside and are absorbed by the cell.

EQE isestimated via formula 4.3.

$$EQE = \frac{e^{-}/\sec}{photon/\sec} \quad \textbf{(4.3)}$$

IQE is also estimated via formula 4.4.

$$IQE = \frac{e^{-}/\sec}{abs.photon/\sec} \quad \textbf{(4.4)}$$

PV Measurements QEX10 was performed for our quantum efficiency studies. Quantum efficiency experiments were set up to read per 30 nm steps for 0.4 second for per step.

5. RESULTS AND DISCUSSION

In this section, obtained samples were characterized in different aspects. XRD and Raman spectroscopy were used to determine crystal structure of CZTS and CZT(S,Se). Compositional analysis is also important for fabricating ideal CZT(S,Se), which is "Cu poor and Zn rich" structure. EDX results represent composition of annealed and selenized samples at different process conditions. UV visible spectroscopy was also used to investigate the band gap of samples. UV study provide us both determine absobtion of CZTS or CZT(S,Se) and determine band gap of thin films. Band gap determination is also provide us estimation of possible secondary phases of films via changing band gap of CZTS films. Finally, IPCE was used to analyze performance characteristics of CZT(S,Se) cell structure at monochromatic wavelength between 200 nm and 1200 nm.

5.1 X-Ray Diffraction (XRD) Results

Crystal structure of quaternary compound KS structure CZTS has been hard to detect between its possible secondary phases. Binary, ternary and quaternary secondary phases of CZTS can occur during reaction and annealing process, so determining crystal structure of CZTS in KS is so important for ideal kesterite structure to be used as an absorber layer in thin film solar cell structure. XRD was used to determine the kesterite structure of CZTS and CZTSSe to be used as an absorber layer.

Figure 5.1 shows that XRD result of as-synthesized CZTS film coated via CZTS ink. CZTS ink was deposited on soda lime glass via spin coating for structural characterization tests determined in section 4. Then the samples were dried at 150 ^{o}C to remove residual organics like toluene used to make a stable ink of CZTS. The result peaks were well matched with literature (JCPDS 01-075-4122) [53, 67]. Main peaks are broad because they are formed at nano size grains and include organic compounds in structure. Initial CZTS crystal has formed at nano size with usage of OLA as a surfactant during reaction.

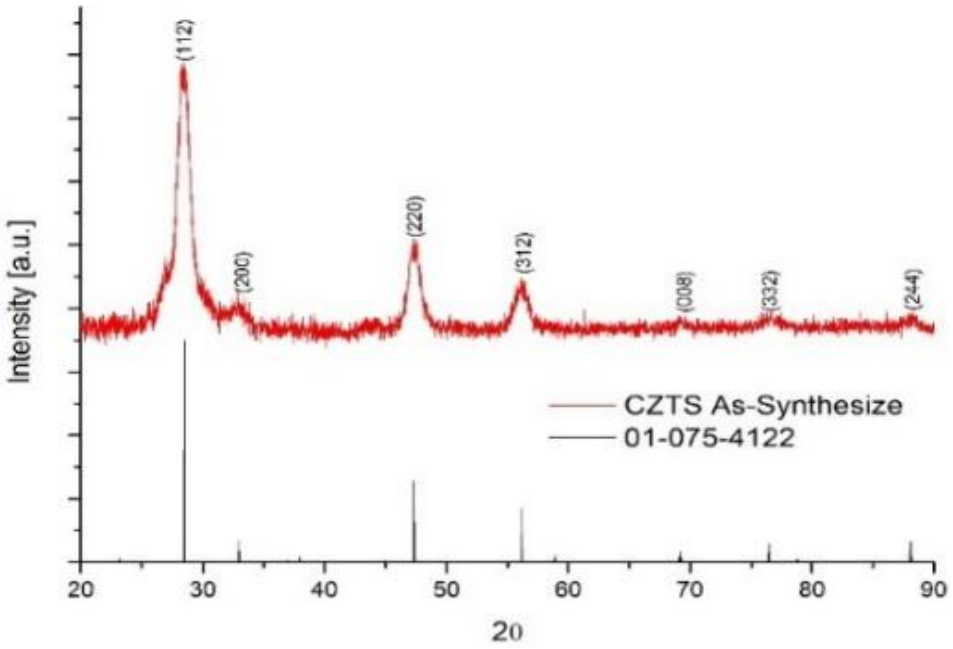

Figure 5.1 : XRD result of CZTS as-synthesised film on SLG substrate.

X-ray diffraction results of annealed samples between 350 ^{o}C and 425 ^{o}C are shown in Figure 5.2. The xrd result of as-synthesis CZTS sample was also given in Figure 5.2 to compare with annealed samples. Maximum intensity peaks were achieved with annealed samples at 400 ^{o}C with high crystallinity in inert gas atmosphere, but some secondary peaksrelated secondary phases of CZTS, which are close the main peak are shown in the structure of the film. Peak intensity of CZTS film that were annealed at 350 and 375 ^{o}C decreased and peak widths were also broaded during annealed process. Evaporated OLA in structure might cause CZTS grains to recrystallizate during annealing process at 350 and 375 ^{o}C. Increasing annealing temperature from 375 to 400 ^{o}C caused crystal growth via given energy at this temperature. Therefore, annealed samples at 350 ^{o}C and 375 ^{o}C were best results for kesterite structure according to position of peaks at two teta althought intensity rates of peaks decreased when it compared xrd result of annealed sample at 400 ^{o}C. However, secondary peaks of CZTS has similar XRD results with kesterite crystal structure according to XRD results.

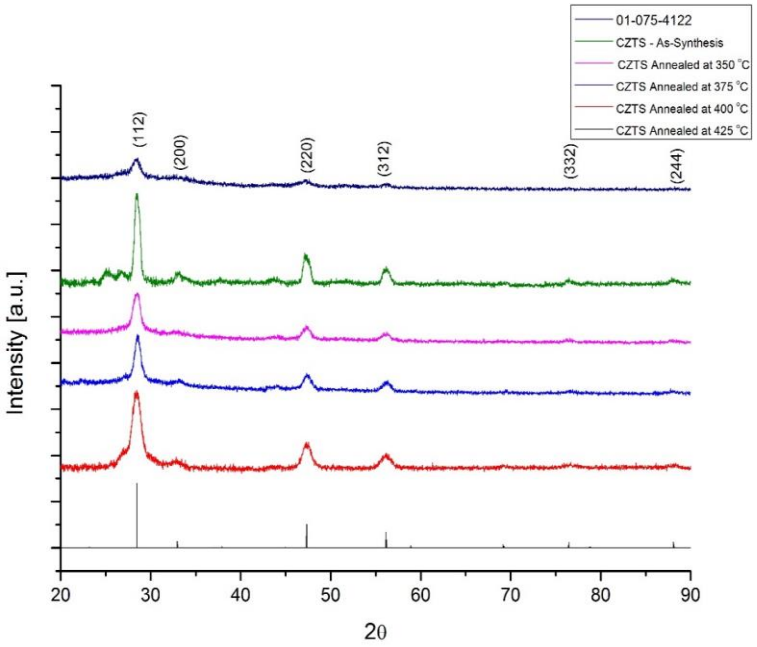

Figure 5.2 : XRD result of annealed CZTS thin film on SLG substrate.

Not only main three peaks of CZTS but also peaks having low intensity related CZTS are shown in Figure 5.3. We have to confirm that this XRD result of CZTS, but presence of low peak of CZTS can be evidence to kesterite structure.

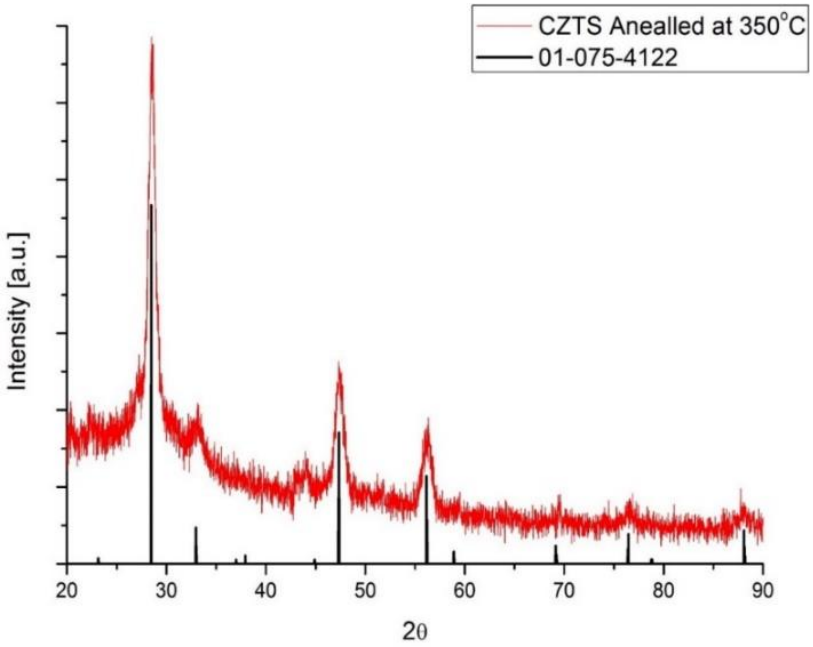

Figure 5.3 : XRD result of annealed CZTS thin film annealed at 350 ^{o}C.

XRD result of selenized samples at 500 ^{o}C for forty minutes matches with literature in terms of broad peaks range, which related to low crystalinity and amorphous structure. There are also some peaks, which were related to reaction between silicon, and selenium during the selenization process is marked as hasahtag in Figure 5.4.

XRD results of selenized samples show that kesterite structure CZTSSe achieved at 500 ^{o}C for forty minutes with low crystallinity structure.

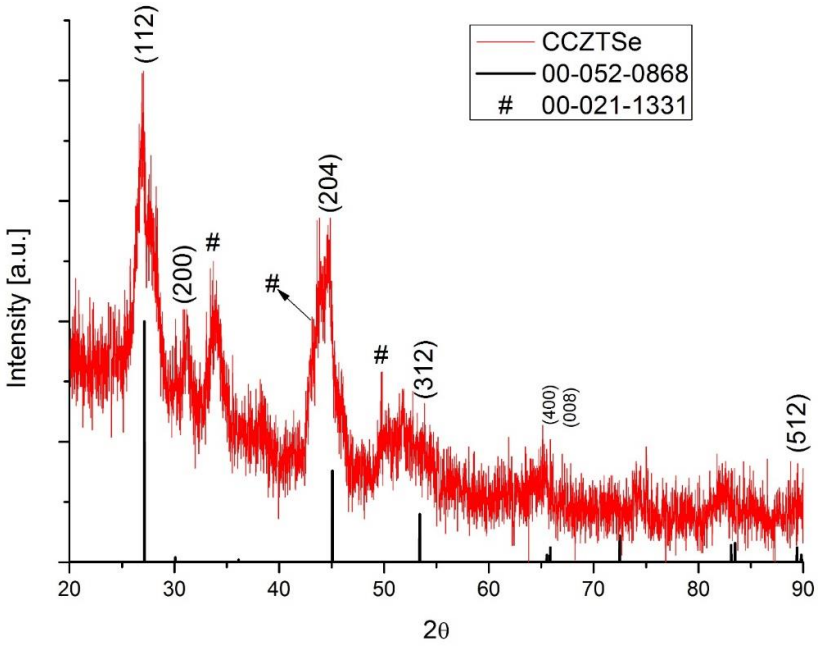

Figure 5.4 : XRD results of slenized CZTSSe thin film.

5.2 Raman Spectroscopy Result

Secondary phases of kesterite structure of quaternary CZTS and the by products such as ZnS and Cu_2SnS_3 have x-ray peaks at the same two theta values [68, 69]. Therefore, XRD results have to be confirmed by Raman spectroscopy [70]. To do that, Raman spectroscopy was used and Raman results make distinguish between these phases and kesterite crystal structure CZTS.

Raman result of as-synthesized CZTS film confirms in Figure 5.5 that the results of XRD studies. Both results are well matched with literature [70]. It can be said that as synthesized CZTS has had kesterite structure. In other words, kesterite structure occurred during the reaction between precursors via adopting surfactant OLA. Figure 5.5 shows that Raman spectroscopy result of as-synthesized CZTS film on soda lime glass substrate. CZTS shifts are shown at 288, 337 360 and 375 cm^{-1}, respectively [71]. Shifts around 288 and 337 cm^{-1} are related with kesterite crystal structure of CZTS while shoulder at 352 and 375 cm^{-1} has not clearly been known that why they appeared in raman spectroscopy results [70].

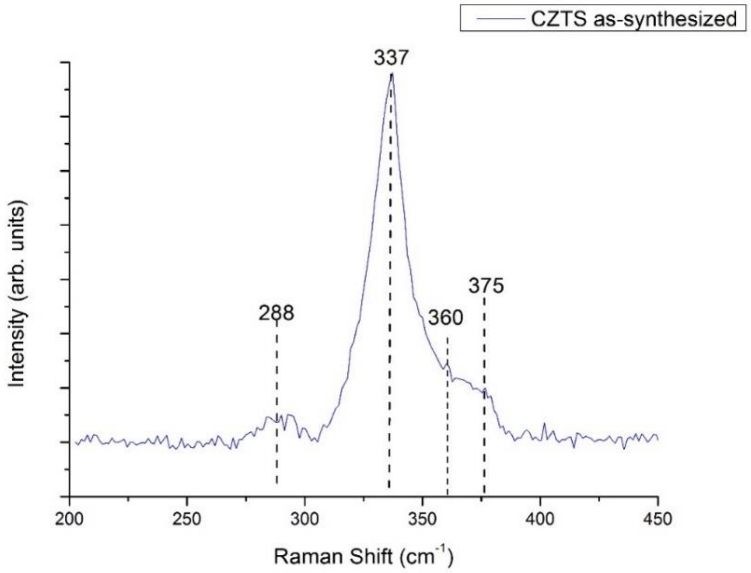

Figure 5.5 : Raman spectroscopy result of as-synthesized CZTS thin film.

Main shift of CZTS having KS crystal structure has changed between 336 and 338 cm^{-1} in Figure 5.6. Annealed samples at 350 ºC and 375 ºC matched with literature as well as XRD results of them. Raman result of annealed sample at 350 ºC also includes all the shifts which are related CZTS structure in Figure 5.6. As seen from Figure 5.4, additional of kesterite structure, secondary phases of CZTS, which was seen in XRD result, can be related position change of shoulder at 375 cm^{-1} for annealed sample at 400 ºC. Raman shifts of annealed sample at 425 ºC disappeared, so composition of Kesterite type CZTS almost complately break down at this temperature.

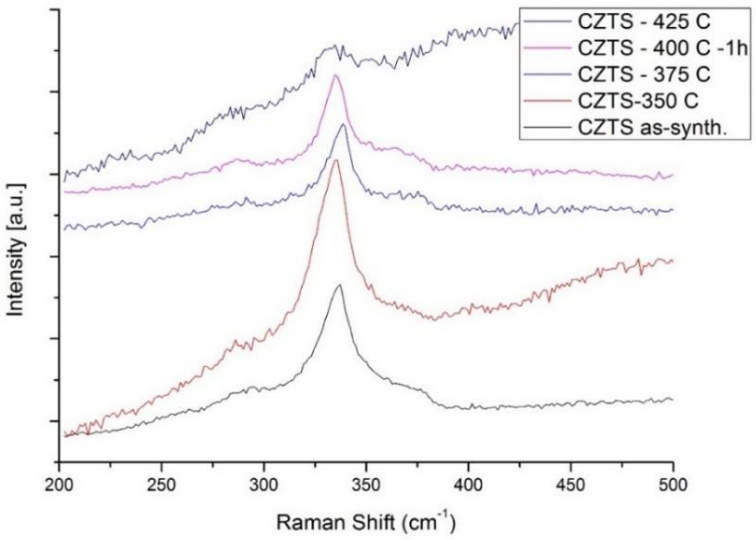

Figure 5.6 : Raman spectroscopy result of annealed CZTS thin films.

5.3 Energy Dispersion X-Ray Spectroscopy (EDX) Results

Not only crystal structure but also composition of CZTS is important for ideal CZTS using as an absorber layer in thin film solar module. The highest power conversion efficiencies by using CZTS as an absorber layer has been achieved with compositions having copper-poor and zinc-rich structures when oleylamine has been used as a surfactant in hot injection method [58]. Therefore, EDX helped us to determine composition of elements in kesterite CZTS and CZT(S,Se) structure. Table 5.1 shows EDX results of as-synthesis and annealed samples.

EDX results show that increasing annealing temperature caused Cu composition in structure to increase while composition of Zn and Sn have decreased which is shown in Table 5.1. The reason of that situation is having lower melting points of Zn and Sn (419 and 231 ^{o}C, respectively) than that of Cu (1084 ^{o}C). Therefore, composition rate of Cu versus Zn+Sn increases while composition rate of Zn versus Sn decreases.

Table 5.1 : Composition rate of annealed CZTS samples at different temperature.

Samples	Cu/Zn+Sn	Zn/Sn	S/Cu+Zn+Sn
As-synthesized	0.78	1,18	1,02
Annealed 350 ^{o}C	0.88	1,15	0,68
Annealed 375 ^{o}C	0.93	1,4	0,71
Annealed 400 ^{o}C	0.95	1,11	0,79

Annealed samples at 350 ^{o}C for an hour in inert atmosphere is shown the best favorable crystal structure and elemental composition for ideal CZTS to be used as an absorber layer in thin film module according to the results of XRD, Raman spectroscopy and EDX.

EDX result of selenized samples is shown in Table 5.2. EDX results belong to selenized samples at different conditions. Samples that have been selenized at 500 ^{o}C for 20 and 40 minutes, 550 ^{o}C for 40 minutes, respectively. EDX results also illustrate that the kinetics of selenization process depend on temperature and duration time. EDX results prove that increasing selenization time from 20 to 40 minutes and temperature from 500 ^{o}C to 550 ^{o}C caused composition of Cu to increase while decreasing of Sn composition. Composition of Zn did not change significantly at 500 ^{o}C selenization temperature. However, increasing temperature from 500 ^{o}C to 550 ^{o}C causes Zn composition to decrease sharply.

Table 5.2 : EDX result of slenized samples at different conditions.

Selenization Conditions	EDX [at. %]				
	Cu	Zn	Sn	S	Se
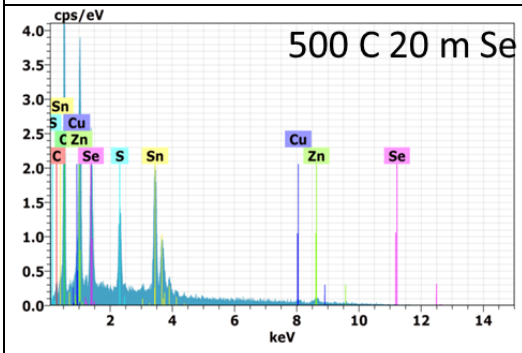	4,5	16,8	35,7	21,6	21,2
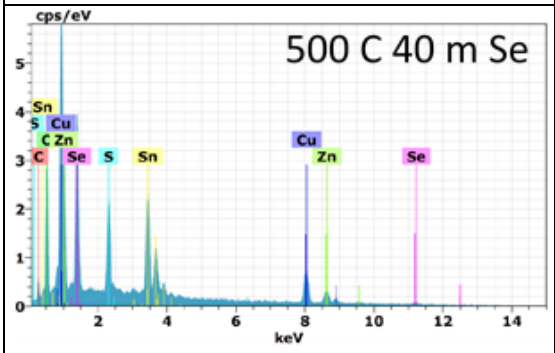	33,8	16,8	17,4	13,5	18,3
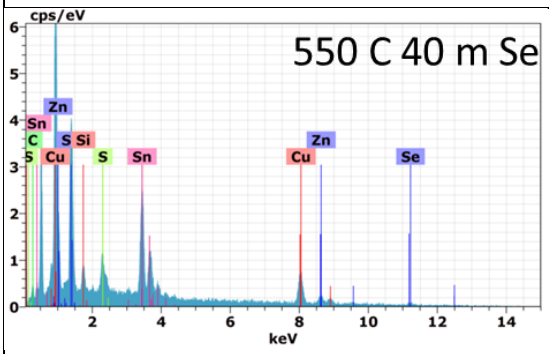	55,1	5,44	10,9	0,07	28,4

Selenized samples at 500 ºC for 20 minutes presents equal amount of sulfur and selenium, while selenized samples at 500 ºC for 40 minutes presents higher Se amount than that of S. This result proves that Se rate depends on duration time of selenization process. Finally, selenized samples at 550 ºC only include selenium in structure. Composition of total anion including total of S and Se decreased with increasing duration and temperature. Temperature and duration are important factors for replacing of sulphur atoms with selenium atoms in CZTS structure. Kinetics of selenization process are important to achieve forming CZT(S,Se) film structure. Therefore, selenization temperature and selenization duration are main factors. Ideal selenization condition should include high crystallinity and high selenium

concentration and low sulphur concentration to adjust bandgap of absorber layer to be used as an absorber layer in thin film solar cell syructure.

EDX result and composition of selenized sample at 550 ºC for 40 minutes at different point of surface are shown in Table 5.3. Binary secondary phase on surface was shown a form of ball shape structure on surface. Formed shape on surface separated on surface homegenously and these forms only included copper and selenium composition according to EDX result, which may be related Cu_2Se phase. Other part of film included Cu, Zn, Sn and Se composition although the composition of it included high Cu and low Zn phase which is not favorable for ideal CZTS for using as an absorber layer in thin film solar module. Over given energy during selenization process caused to form stable Cu_2Se phase on surface kinetically.

Table 5.3 : EDX points and composition of selenized samples at 550 ºC for 40 min.

EDX Point	EDX [at. %]				
	Cu	Zn	Sn	S	Se
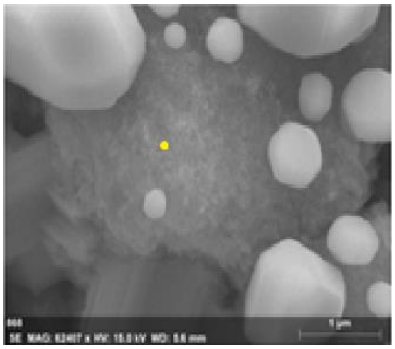	38,58	10,50	21,12	0,12	22,72
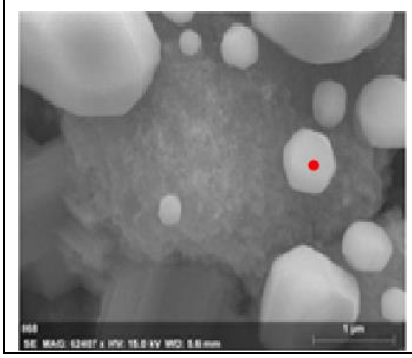	67,89	-	-	-	32,11

5.4 Scanning Electron Microscopy (SEM) Results

SEM images of annealed CZTS and selenized CZTSSe samples are shown Figure 5.7. SEM images indicated that some fructure on film surface of annealed samples was generated. Organics in film structure during annealing process have lead to

fracture because evaporated organics have cracked film surface to diffuse away from structure. Fructures on surface have spreaded throughout the surface regularly.

It can be clearly seen that after selenization process, quality of film surface has increased. Cracks on surface of annealed samples were disappeared during the selenization process when selenium partially took place sulfur. Selenization process makes possible not only adjust band gap of CZTS film but also increases the surface quality of films. However, surface of CZTSSe is still porous.

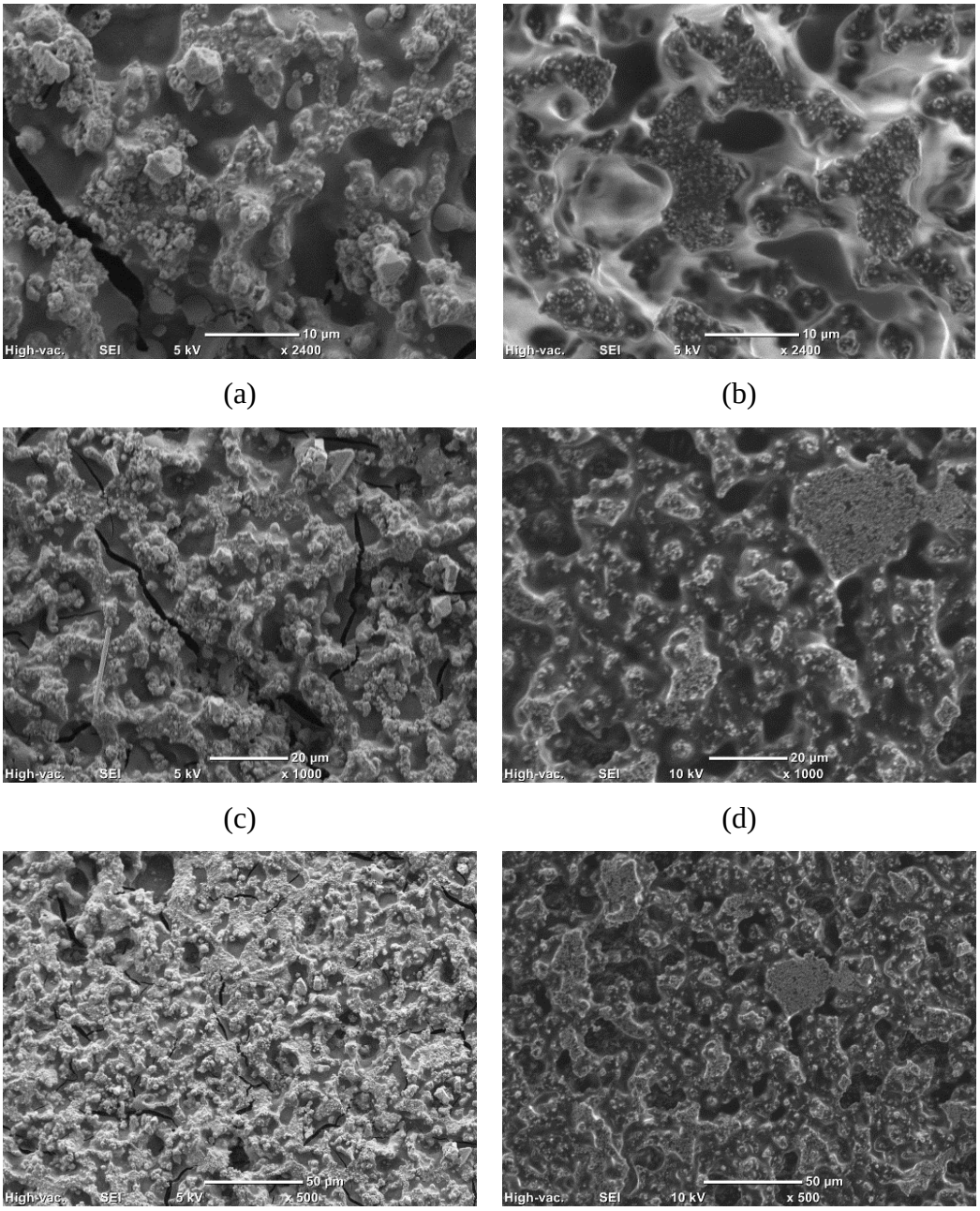

Figure 5.7 : SEM images of annealed CZTS (a), (c) and (e) and selenized CZTSSe (b), (d) and (f).

5.5 UV-Visible Spectroscopy Results

Band gap of synthesized CZTS was estimated at 1.5 eV as a result of normalizing slope of graphic $(\alpha h\nu)^2$ versus $(h\nu)$ in Figure 5.8. Slope of result graphic is intersected at 1.5 eV. Band gap result of as-synthesized samples is well matched with literature of kesterite crystal structure CZTS.

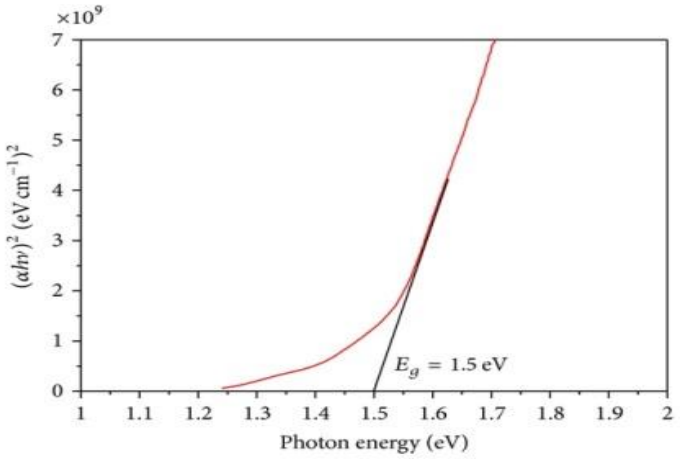

Figure 5.8 : $(\alpha h\nu)^2$ versus $h\nu$ graphic of as-synthesized CZTS.

Bandgap of selenized samples at 500 ºC for 40 minutes was calculated around 1.14 eV according to transmission result in Figure 5.9. The x ratio in CZT(S_xSe_{1-x}) can be estimated as a result of band gap (Figure 3.8). Band gap of CZTS is 1.5 eV while band gap of CZTSe is 1.14 eV. According to Figure 3.8, ratio between Se and S can be estimated as 2,57.

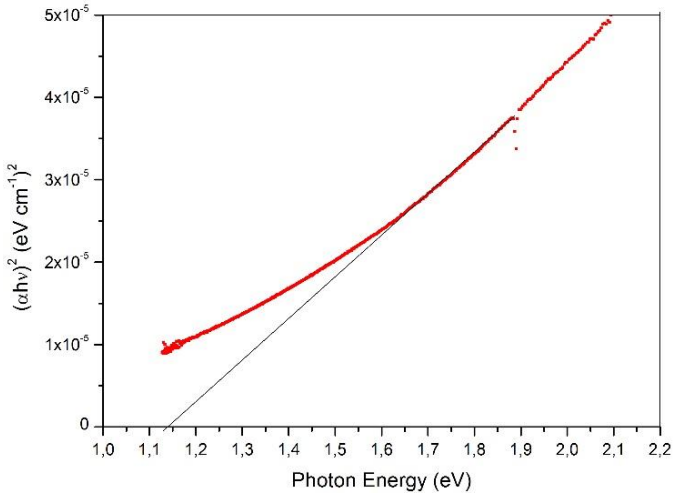

Figure 5.9 : $(\alpha h\nu)^2$ versus $h\nu$ graphic of selenized CZTSSe at 500 ºC for 40 minutes.

5.6 External Quantum Efficiency (EQE) Analysis

Figure 5.10 shows that the external quantum efficiency (EQE) curve of the best photovoltaic cells from samples of CZTS that has been annealed at 350 ^{o}C for an hour in inert gas atmosphere and coated onto Molybdenum coated glass substrate. The highest EQE is around 43 % at 600 nm.

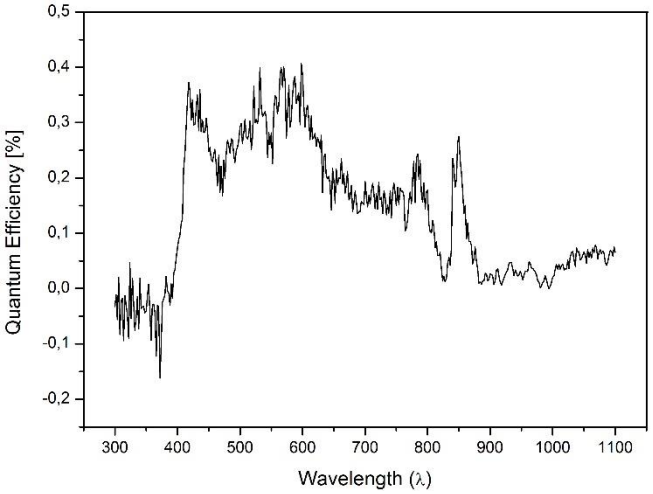

Figure 5.10 : EQE of Mo/CZTS/PCBM/Ag hybrid PV cell structure.

6. CONCLUSIONS AND RECOMMENDATIONS

In this study, Cu_2ZnSnS_4/Se_4 quaternary compound was synthesized via hot injection method. Metal precursors (copper (II) acetylacetonate, zinc acetylacetonate, tin (IV) acetylacetonate dibromide) were added into oleylamine and also sulfur was added oleylamine in another flask. Then solutions were mixed and it was waited an hour to complete the reactions between them. After that, as received solution was washed and centrifuged with toluene and IPA to obtain pure CZTS ink. Finally toluene was filled to final supetanant of CZTS to make a stable CZTS ink. Different precursor and precursor ratios were also tried to optimize the synthesis.

CZTS ink were coated onto soda lime glass, molybdenum coated glass and molybdenum foil via either spin coating or drop casting methods to obtain CZTS films. These films were annealed at different temperatures and times in inert N_2 atmosphere to increase crystallinity and remove organics in structure. Then films were selenized at different temperatures for different times. Characterization tests were performed both before and after annealing and selenization process to gain information about crystal structure, morphology, electrical properties, optical properties of CZTS material.

X-ray diffraction and Raman spectroscopy were used to obtain crystal structure of the as received substrates. These results have shown that the substrates are kesterite CZTS quaternary material. Some secondary peaks related to silicon, selenium and molybdenum were observed after selenization. These results have also shown that optimum annealing temperature was around 350 and 375 ^oC. After 400 ^oC, crystal structures completely broke down.

UV-vis spectroscopy studies were performed to investigate absorption behaviors and band gap of substrates. Band gap of CZTS ink is around 1.5 eV which is matched with the literature. After selenization process, band gap of films were around 1.14 eV.

Scanning electron microscope have shown that films are uniform and continuous. EDX results have revealed that structure is copper poor zinc rich. This result shows a good stoichiometry for a high efficient solar cell device for later studies. After selenization process, it was seen from the EDX results that selenium was successfully deposited into the substrate for some conditions.

To conclude that, xxx mmol copper (II) acetylacetonate, xxx mmol zin acetylacetonate, xxx mmol tin (IV) bisacetylacetonate dibromide and xxx mmol sulfur are the best amounts of precursors for good stoichiometry. Also xxx ml oleylamine was used as surfactant. Also annealing at 350 or 375 ^{o}C at N_2 atmosphere is good for the removing residual organics in the structure. For selenization process, 500 ^{o}C for 40 minutes is good for the obtain CZTSe material for an effective solar cell device.

REFERENCES

[1] **H. Flammersberger,** (2010) Experimental study of Cu_2ZnSnS_4 thin films for solar cells, Uppsala University.

[2] **Kopetz, Heinz.** (2013) Renewable resources: Build a biomass energy market. Nature 494.7435: 29-31**.**

[3] **Cowan, Robin.** (1990) Nuclear power reactors: a study in technological lock-in. The journal of economic history 50.03: 541-567.

[4] **C. A. Wolden, J. Kurtin, J. B. Baxter, I. Repins, S. E. Shaheen, 1. T. Torvik et aI**, (2011) "Photovoltaic manufacturing: Present status, future prospects, and research needs," 1. Vac. Sci. Teclmol. A, vol. 29, no. 3, pp. 030801-1- 030801-16.

[5] **Green, Martin A.** (1987) High efficiency silicon solar cells. Seventh EC Photovoltaic Solar Energy Conference. Springer Netherlands.

[6] **S. Plaza.** (2011, Aug.) Top 10 World's Most Efficient Solar PY Modules (Poly-Crystalline) [Online]. Available: http: //www.solarplaza.com/topl0-polycrystalline-module-efficiency.

[7] **P. Jackson, D. Hariskos, E. Lotter, S. Paetel, R. Wuerz, R. Menner et aI.**, (2011, Nov.) "New world record efficiency for $Cu(In,Ga)Se_2$ thin-film solar cells beyond 20%," Progr. Photovoltaics, vol. 19, pp. 894-897.

[8] **A. Chirilii, S. Buecheler, F. Pianezzi, P. Bloesch, C. Gretener, A. R. Uhl et aI.**, (2011, Sep.) Highly efficient $Cu(In,Ga)Se_2$ solar cells grown on flexible polymer films, Nat. Mater., vol. 10, pp. 857-861.

[9] **M.-O. Ruault, O. Kaitasov, R. Triboulet, J. Crestou, M. Gasgnier,** (1994) Journal of Crystal Growth, 143, pp. 40-45.

[10] **P. Jackson, D. Hariskos, E. Lotter, S. Paetel, R. Wuerz, R. Menner, W. Wischmann, M. Powalla**, (2011) Progress In Photovoltaics: Research and Applications 19, pp. 894–897.

[11] **K. Ramasamy, M. A. Malik and P. O'Brien**, (2012) Routes to copper zinc tin sulfide Cu_2ZnSnS_4 a potential material for solar cells," Chem. Commun. 48, 5703-5714.

[12] **I.D. Olekseyuk, I.V. Dudchak, L.V.** (2004) Piskach, Journal of Alloys and Compounds 368, pp. 135-143.

[13] **A. Walsh, S. Chen, S.-H Wei, X.-G. Gong**, (2012) Advanced Energy Materials, 2, pp. 400-409.

[14] **Shibata, T., Muranushi, Y., Miura, T., & Kishi, T.** (1991). Chemical and structural characterization of SnS2 single crystals grown by low-temperature chemical vapour transport. Journal of materials science, 26(18), 5107-5112.

[15] **Hwang, Y., Park, B. I., Lee, B. S., Kim, J. Y., Jeong, J. H., Kim, H., Lee, D. K.** (2014). Influences of Extended Selenization on $Cu_2ZnSnSe_4$ Solar Cells Prepared from Quaternary Nanocrystal Ink. The Journal of Physical Chemistry C, 118(48), 27657-27663.

[16] **T. Tanaka, T. Nagatomo, D. Kawasaki, M. Nishio, Q.X. Guo, A. Wakahara, A. Yoshida, H. Ogawa,** (2005) J. Phys. Chem. Solids 66 1978–1981.

[17] **T. Kobayashi, K. Jimbo, K. Tsuchida, S. Shinoda, T. Oyanagi, H. Katagiri,** (2005) Jpn. J. Appl. Phys. 44 783–787.

[18] **Redinger, A., & Siebentritt, S.** (2010). Coevaporation of $Cu_2ZnSnSe_4$ thin films. Applied Physics Letters, 97(9), 092111.

[19] **R.A. Wibowo, E.S. Lee, B. Munir, K.H. Kim,** (2007) Phys. Status Solidi A 204 3373–3379.

[20] **F. Yakuphanoglu,** (2011) Sol. Energy 85 (2011) 2518–2523.

[21] **Mali, Sawanta S., et al.** (2012), Synthesis and characterization of Cu_2ZnSnS_4 thin films by SILAR method, Journal of Physics and Chemistry of Solids 73.6 (2012): 735-740.

[22] **Todorov, T. K., Tang, J., Bag, S., Gunawan, O., Gokmen, T., Zhu, Y., & Mitzi, D. B.** (2013). Beyond 11% efficiency: characteristics of state-of-the-art $Cu_2ZnSn(S,Se)_4$ solar cells. Advanced Energy Materials, 3(1), 34-38.

[23] **H. Katagiri, K. Jimbo, W.S. Maw, K. Oishi, M. Yamazaki, H. Araki, A. Takeuchi,** (2009) Thin Solid Films 517 2455–2460.

[24] **W. Wang, M.T. Winkler, O. Gunawan, T. Gokmen, T.K. Todorov, Y. Zhu, D.B. Mitzi,** (2014) Device characteristics of CZTSSe thin-film solar cells with 12.6% efficiency, Adv. Energy Mater. 4 1301465.

[25] **Jackson, P., Hariskos, D., Lotter, E., Paetel, S., Wuerz, R., Menner, R., Powalla, M**. (2011). New world record efficiency for $Cu(In,Ga)Se_2$ thin-film solar cells beyond 20%. *Progress in Photovoltaics: Research and Applications*,*19*(7), 894-897.

[26] **Bhattacharya, R. N., & Ramanathan, K.** (2004). $Cu(In,Ga)Se_2$ thin film solar cells with buffer layer alternative to CdS. Solar Energy, 77(6), 679-683.

[27] **Wang, W., Winkler, M. T., Gunawan, O., Gokmen, T., Todorov, T. K., Zhu, Y., & Mitzi, D. B.** (2014). Device Characteristics of CZTSSe Thin-Film Solar Cells with 12.6% Efficiency. Advanced Energy Materials, 4(7).

[28**] Ito K. and Nakazawa T.,** (1988) Electrical and optical properties of stannite-type quaternary semiconductor thin films, Japanese Journal of Applied Physics, 27, 2094–2097.

[29] **T. M. Friedlmeier, N. Wieser, T. Walter, H. Dittrich, and H. W. Schock,** (1977), Heterojuncitons based on Cu_2ZnSnS_4 and $Cu_2ZnSnSe_4$ thin films," in Proceedings of the 14th European Conference of Photovoltaic Science and Engineering and Exhibition, p. 1242, Bedford, UK.

[30] **H. Katagiri, K. Saitoh, T. Washio, H. Shinohara, T. Kurumadani, and S. Miyajima,** (2001), Development of thin film solar cell based on Cu_2ZnSnS_4 thin films, Solar Energy Materials and Solar Cells, 65, 141–148.

[31] **H. Katagiri, K. Jimbo, S. Yamada et al.,** (2008) "Enhanced conversion efficiencies of Cu_2ZnSnS_4-based thin film solar cells by using preferential etching technique," Applied Physics Express, 1, Article ID 041201.

[32] **H. Katagiri, K. Jimbo, W. S. Maw et al.,** (2009) "Development of CZTS-based thin film solar cells," Thin Solid Films, 517, 2455–2460.

[33] **Todorov, T. K., Reuter, K. B., & Mitzi, D. B.** (2010). High-Efficiency Solar Cell with Earth-Abundant Liquid-Processed Absorber. Advanced materials, 22(20), E156-E159.

[34] **Hummelen, Jan C.; Knight, Brian W.; Lepeq, F.; Wudl, Fred; Yao, Jie; Wilkins, Charles L.** (1995). "Preparation and Characterization of Fulleroid and Methanofullerene Derivatives". The Journal of Organic Chemistry 60 (3): 532–538. doi:10.1021/jo00108a012.

[35] **J. S. Seol, S. Y. Lee, J. C. Lee, H. D. Nam, and K. H. Kim,** (2003) "Electrical and optical properties of Cu_2ZnSnS_4 thin films prepared by rf magnetron sputtering process," Solar Energy Materials and Solar Cells, 75, 155–162.

[36] **T. Tanaka, T. Nagatomo, D. Kawasaki et al.,** Preparation of Cu_2ZnSnS_4 thin films by hybrid sputtering, Journal of Physics.

[37] **F. Y. Liu, K. Zhang, Y. Q. Lai, J. Li, Z. A. Zhang, and Y. X. Liu,** (2010) "Growth and characterization of Cu_2ZnSnS_4 thin films by dc reactive magnetron sputtering for photovoltaic applications," Electrochemical and Solid-State Letters, 13, H379–H381..

[38] **H. Katagiri, N. Sasaguchi, S. Hando, S. Hoshino, J. Ohashi, T. Yokota,** (1997) Preparation and evaluation of Cu_2ZnSnS_4 thin films by sulfurization of E-B evaporated precursors, solar Energy Materials & Solar Cells, 49 407-414.

[39] **H. Katagiri, K. Saitoh, T. Washio, H. Shinohara, T. Karumadani, S. Miyajima,** (2001), Development of thin film solar cell based on Cu_2ZnSnS_4 thin films, solar Energy Materials & Solar Cells, 65 141-148.

[40] **T. Kobayashi, K. Jimbo, K. Tsuchida, S. Shinoda, T. Oyanagi, H. Katagiri,** (2005), Investigation of Cu_2ZnSnS_4-Based Thin Film Solar Cells Using Abundant Materials, Japanese Journal of Applied Physics, 44 783-787.

[41] **K. Wang, O. Gunawan, T. Todorov, B. Shin, S.J. Chey, N.A. Bojarczuk, D. Mitzi, S. Guha,** (2010), Thermally evaporated Cu_2ZnSnS_4 solar cells, Applied Physics Letters, 97 (2010) 143508.

[42] **B. Shin, O. Gunawan, Y. Zhu, N.A. Bojarczuk, S.J. Chey, S. Guha,** (2013), Thin film solar cell with 8.4% power conversion efficiency using an earth-abundant Cu_2ZnSnS_4 absorber, Progress in Photovoltaics: Research and Applications, 21 (2013) 72-76.

[43] **B. Shin, Y. Zhu, N.A. Bojarczuk, S. Jay Chey, S. Guha,** (2012) Control of an interfacial $MoSe_2$ layer in $Cu_2ZnSnSe_4$ thin film solar cells: 8.9% power conversion efficiency with a TiN diffusion barrier, Applied Physics Letters, 101(5) 053903.

[44] **D. B. Chrisey and G. K. Hubler,** (1994), Pulsed laser deposition of thin films, 14, New York, John Wiley and Sons.

[45] **H.U. Krebs, M. Weisheit, J. Faupel, E. Suske, T. Scharf, C. Fuhse, M. Stormer, K. Sturm, M. Seibt, H. Kijewski, E. Panchenko and M. Buback,** (2003), Pulsed laser deposition (PLD) – A versatile thin film technique," Adv. Solid State Phys., 43, 101–107.

[46] **K. Sekiguchi, K. Tanaka, K. Moriya and H. Uchiki,** (2006), Epitaxial growth of Cu_2ZnSnS_4 thin films by pulsed laser deposition, Phys. Stat. Sol. C., 3C, (8), 2618–2621.

[47] **K. Moriya, K. Tanaka and H. Uchiki,** (2007) Fabrication of Cu_2ZnSnS_4 thin-film solar cell prepared by pulsed laser deposition, Jpn J. Appl. Phys., 46, 5780–5781.

[48] **J.J. Scragg, P.J. Dale, L.M. Peter, G. Zoppi, I. Forbes,** (2008), New routes to sustainable photovoltaics: evaluation of Cu_2ZnSnS_4 as an alternative absorber material, Physica Status Solidi (b), 245 (2008) 1772-1778.

[49] **J.J. Scragg, D.M. Berg, P.J. Dale,** (2010), A 3.2% efficient Kesterite device from electrodeposited stacked elemental layers, Journal of Electroanalytical Chemistry, 646 (2010) 52-59.

[50] **S. Ahmed, K.B. Reuter, O. Gunawan, L. Guo, L.T. Romankiw, H. Deligianni,** (2012) A High Efficiency Electrodeposited Cu_2ZnSnS_4 Solar Cell, Advanced Energy Materials, 2 (2012) 253-259.

[51] **K. Tanaka, M. Oonuki, N. Moritake, H. Uchiki,** (2009), Cu_2ZnSnS_4 thin film solar cells prepared by non-vacuum processing, Solar Energy Materials & Solar Cells, 93 583-587.

[52] **K. Tanaka, Y. Fukui, N. Moritake, H. Uchiki,** (2011), Chemical composition dependence of morphological and optical properties of Cu_2ZnSnS_4 thin films deposited by sol–gel sulfurization and Cu_2ZnSnS_4 thin film solar cell efficiency, Solar Energy Materials & Solar Cells, 95 838-842.

[53] **Q. Guo, H. W. Hillhouse and R. Agrawal,** (2009), Synthesis of Cu_2ZnSnS_4 nanocrsytal ink and its use for solar cells, J. Am. Chem. Soc., 131, 12054.

[54] **Steinhagen, C., Panthani, M. G., Akhavan, V., Goodfellow, B., Koo, B., & Korgel, B. A.** (2009). Synthesis of Cu_2ZnSnS_4 nanocrystals for use in low-cost photovoltaics. Journal of the American Chemical Society, 131(35), 12554-12555.

[55] **Ki, W., & Hillhouse, H. W.** (2011). Earth-Abundant Element Photovoltaics Directly from Soluble Precursors with High Yield Using a Non-Toxic Solvent. Advanced Energy Materials, 1(5), 732-735.

[56] **Fella, C. M., Uhl, A. R., Romanyuk, Y. E., & Tiwari, A. N.** (2012). $Cu_2ZnSnSe_4$ absorbers processed from solution deposited metal salt precursors under different selenization conditions. physica status solidi (a), 209(6), 1043-1048.

[57] **Guo, Q., Ford, G. M., Yang, W. C., Walker, B. C., Stach, E. A., Hillhouse, H. W., & Agrawal, R.** (2010). Fabrication of 7.2% efficient CZTSSe solar cells using CZTS nanocrystals. Journal of the American Chemical Society, 132(49), 17384-17386.

[58] **Miskin, C. K., Yang, W. C., Hages, C. J., Carter, N. J., Joglekar, C. S., Stach, E. A., & Agrawal, R.** (2014). 9.0% efficient $Cu_2ZnSn(S, Se)_4$ solar cells from selenized nanoparticle inks. Progress in Photovoltaics: Research and Applications.

[59] **Schorr, S.** (2011). The crystal structure of kesterite type compounds: A neutron and X-ray diffraction study. Solar Energy Materials and Solar Cells, 95(6), 1482-1488.

[60] **Chen, S., Gong, X. G., Walsh, A., & Wei, S. H.** (2009). Crystal and electronic band structure of Cu_2ZnSnX_4 (X= S and Se) photovoltaic absorbers: first-principles insights. Applied Physics Letters, 94(4), 041903-041903.

[61] **Paier, J., Asahi, R., Nagoya, A., & Kresse, G.** (2009). Cu_2ZnSnS_4 as a potential photovoltaic material: a hybrid Hartree-Fock density functional theory study. Physical Review B, 79(11), 115126.

[62] **Hall, S. R., Szymanski, J. T., & Stewart, J. M.** (1978). Kesterite, Cu< 2)(Zn, Fe) SnS< 4), and stannite, Cu< 2)(Fe, Zn) SnS< 4), structurally similar but distinct minerals. The Canadian Mineralogist, 16(2), 131-137.

[63] **Magri, R., Wei, S. H., & Zunger, A.** (1990). Ground-state structures and the random-state energy of the Madelung lattice. Physical Review B, 42(17), 11388.

[64] **Bernard, J. E., Ferreira, L. G., Wei, S. H., & Zunger, A.** (1988). Ordering of isovalent intersemiconductor alloys. Physical Review B, 38(9), 6338.

[65] **Liu, H. R., Chen, S., Zhai, Y. T., Xiang, H. J., Gong, X. G., & Wei, S. H.** (2012). First-principles study on the effective masses of zinc-blend-derived $Cu_2Zn- IV- VI_4$ (IV= Sn, Ge, Si and VI= S, Se). Journal of Applied Physics, 112(9), 093717.

[66] **Walsh, A., Chen, S., Wei, S. H., & Gong, X. G.** (2012). Kesterite Thin-Film Solar Cells: Advances in Materials Modelling of Cu_2ZnSnS_4. Advanced Energy Materials, 2(4), 400-409.

[67] **Li, C., Cao, M., Huang, J., Wang, L. J., & Shen, Y.** (2015). Mechanism study of structure and morphology control of solvothermal synthesized Cu_2ZnSnS_4 nanoparticles by using different sulfur precursors. Materials Science in Semiconductor Processing, 31, 287-294.

[68] **Dale, P. J., Hoenes, K., Scragg, J., & Siebentritt, S.** (2009, June). A review of the challenges facing kesterite based thin film solar cells. In Photovoltaic Specialists Conference (PVSC), 2009 34th IEEE (pp. 002080-002085). IEEE.

[69] **Gurav, K. V., Pawar, S. M., Shin, S. W., Agawane, G. L., Patil, P. S., Moon, J. H., Kim, J. H.** (2013). Electrosynthesis of CZTS films by sulfurization of CZT precursor: Effect of soft annealing treatment. Applied Surface Science, 283, 74-80.

[70] **Fernandes, P. A., Salomé, P. M. P., & Da Cunha, A. F.** (2011). Study of polycrystalline Cu_2ZnSnS_4 films by Raman scattering. Journal of Alloys and Compounds, 509(28), 7600-7606.

[71] **Huang, C., Chan, Y., Liu, F., Tang, D., Yang, J., Lai, Y., Liu, Y.** (2013). Synthesis and characterization of multicomponent Cu 2 (Fe_xZn_{1-x}) SnS4 nanocrystals with tunable band gap and structure. Journal of Materials Chemistry A, 1(17), 5402-5407.

CURRICULUM VITAE

Name Surname	**: Ridvan ERGUN**
Place and Date of Birth	**: Istanbul / 1988**
Address	**: Avcılar / Istanbul**
E-Mail	**: ridvanergunn@gmail.com**
B.Sc.	**: Gebze Institute of Technology**
	Material Science & Engineering (2006-2011)

PUBLICATIONS/PRESENTATIONS ON THE THESIS

- **Ergun R.**, Calli C., Arici E.U**.**, 2015: Synthesis and characterization of CZTS,Se) thin films for photovoltaic applications. *SOLAR-TR-3 Third Turkish Electricity Conference,* April 27-29, 2015 Ankara, Turkey
- **Ergun R.**, Calli C., Arici E.U**.**, 2015: Synthesis and characterization of CZTS,Se) thin films for photovoltaic applications. *DSL Munih – 11th International Conference on Diffusion in Solids and Liquids* June 22-26, 2015 Munih, Germany